Published in final edited form as:

Nat Immunol. 2023 April ; 24(4): 625–636. doi:10.1038/s41590-023-01447-8.

Dectin-1 signaling on colonic γδ T cells promotes psychosocial stress responses

Xiaolei Zhu[1,18], **Shinji Sakamoto**[1,2,18], **Chiharu Ishii**[3], **Matthew D. Smith**[4], **Koki Ito**[1,5], **Mizuho Obayashi**[1], **Lisa Unger**[1,6], **Yuto Hasegawa**[1], **Shunya Kurokawa**[7], **Taishiro Kishimoto**[7,8], **Hui Li**[9,17], **Shinya Hatano**[10], **Tza-Huei Wang**[9], **Yasunobu Yoshikai**[10], **Shin-ichi Kano**[11], **Shinji Fukuda**[3,12,13,14], **Kenji Sanada**[15], **Peter A. Calabresi**[4,16], **Atsushi Kamiya**[1]

[1]Department of Psychiatry and Behavioral Sciences, Johns Hopkins University School of Medicine, Baltimore, MD, USA.

[2]Department of Neuropsychiatry, Okayama University Graduate School of Medicine, Dentistry, and Pharmaceutical Sciences, Okayama, Japan.

[3]Institute for Advanced Biosciences, Keio University, Tsuruoka, Japan.

[4]Department of Neurology, Johns Hopkins University School of Medicine, Baltimore, MD, USA.

[5]Department of Psychiatry, Hokkaido University Graduate School of Medicine, Hokkaido, Japan.

[6]Institute of Neuroimmunology and Multiple Sclerosis, University Medical Centre Hamburg–Eppendorf, Hamburg, Germany.

[7]Department of Neuropsychiatry, Keio University School of Medicine, Tokyo, Japan.

[8]Hills Joint Research Laboratory for Future Preventive Medicine and Wellness, Keio University School of Medicine, Tokyo, Japan.

Correspondence and requests for materials should be addressed to Atsushi Kamiya. akamiya1@jhmi.edu.

Author contributions

X.Z., S.S. and A.K. designed the study. X.Z. and S.S. performed cellular, behavioral and immunohistochemical experiments, and contributed to data analysis for all experiments. K.I., M.D.S., L.U., Y.H. and M.O. assisted X.Z. and S.S. with the cellular, behavioral and histochemical assays. X.Z. and S.S. performed shotgun metagenomic sequencing and analyzed taxonomic data. C.I. and S.F. performed *16S* rRNA gene sequencing and analyzed taxonomic data together with S.S., X.Z. and K.S. S.K., T.K. and K.S. contributed to human data collection and analysis. H.L. and T.-H.W. contributed to the La1 culture, and helped X.Z. and M.O. perform in vivo La1 administration. S.H. and Y.Y. contributed to the production and characterization of antibody to Vγ6 as well as data interpretation of the flow cytometry experiments. P.A.C. and S.-i.K. contributed to study design, data analysis and interpretation, and provided technical assistance in the cellular experiments. A.K. contributed to the concept or design of the work, and drafting the manuscript with X.Z. and S.S. All authors have approved the final manuscript.

Online content

Any methods, additional references, Nature Portfolio reporting summaries, source data, extended data, supplementary information, acknowledgements, peer review information; details of author contributions and competing interests; and statements of data and code availability are available at https://doi.org/10.1038/s41590-023-01447-8.

Reporting summary

Further information on research design is available in the Nature Portfolio Reporting Summary linked to this article.

Competing interests

The authors declare no competing interests.

Extended data is available for this paper at https://doi.org/10.1038/s41590-023-01447-8.

Supplementary information The online version contains supplementary material available at https://doi.org/10.1038/s41590-023-01447-8.

[9]Departments of Mechanical Engineering and Biomedical Engineering, Johns Hopkins University, Baltimore, MD, USA.

[10]Medical Institute of Bioregulation, Kyushu University, Fukuoka, Japan.

[11]Department of Psychiatry and Behavioral Neurobiology, University of Alabama at Birmingham Heersink School of Medicine, Birmingham, AL, USA.

[12]Gut Environmental Design Group, Kanagawa Institute of Industrial Science and Technology, Kawasaki, Japan.

[13]Transborder Medical Research Center, University of Tsukuba, Tsukuba, Japan.

[14]Laboratory for Regenerative Microbiology, Graduate School of Medicine, Juntendo University, Tokyo, Japan.

[15]Department of Psychiatry, School of Medicine, Showa University, Tokyo, Japan.

[16]Department of Neuroscience, Johns Hopkins University School of Medicine, Baltimore, MD, USA.

[17]Present address: School of Electrical, Computer and Biomedical Engineering, Southern Illinois University, Carbondale, IL, USA.

[18]These authors contributed equally: Xiaolei Zhu, Shinji Sakamoto.

Abstract

The intestinal immune system interacts with commensal microbiota to maintain gut homeostasis. Furthermore, stress alters the microbiome composition, leading to impaired brain function; yet how the intestinal immune system mediates these effects remains elusive. Here we report that colonic γδ T cells modulate behavioral vulnerability to chronic social stress via dectin-1 signaling. We show that reduction in specific *Lactobacillus* species, which are involved in T cell differentiation to protect the host immune system, contributes to stress-induced social-avoidance behavior, consistent with our observations in patients with depression. Stress-susceptible behaviors derive from increased differentiation in colonic interleukin (IL)-17-producing γδ T cells (γδ17 T cells) and their meningeal accumulation. These stress-susceptible cellular and behavioral phenotypes are causally mediated by dectin-1, an innate immune receptor expressed in γδ T cells. Our results highlight the previously unrecognized role of intestinal γδ17 T cells in the modulation of psychological stress responses and the importance of dectin-1 as a potential therapeutic target for the treatment of stress-induced behaviors.

Chronic stress induces peripheral and intracerebral immune changes and inflammation, leading to neuropathology and behavioral abnormalities relevant to psychiatric disorders such as depression and anxiety[1-3]. These inflammatory immune changes include alterations in the gut microbiota that are associated with stress-induced behavior outcomes and disease pathophysiology[4]. Multiple peripheral immune and inflammatory factors—such as circulating macrophages, inflammatory cytokines, hormones and extracellular vesicle-associated microRNAs—are recognized as pathological mediators of stress-induced behaviors[1,2,5-7]. However, it is not known how chronic stress alters the intestinal immune system mediating the aberrant gut–brain axis, leading to neurobehavioral consequences.

γδ T cells are unique T lymphocytes that are enriched in peripheral mucosal tissues, including intestines, and mediate innate and adaptive immune responses[8]. Previous studies showed that γδ T cells are involved in the pathophysiology of inflammatory diseases —such as inflammatory bowel disease, lung cancer and brain ischemia—by generating chemotactic signals such as interleukin (IL)-17 in crosstalk with a myeloid series of cells[9-11]. Interestingly, recent studies highlighted the roles of γδ T cells in the meninges for the regulation of brain function. Under steady-state conditions, the meningeal interferon (IFN)-γ-producing T cells are involved in the modulation of social behaviors[12], whereas meningeal-resident IL-17-producing γδ T cells (γδ17 T cells) modulate anxiety-like behavior and memory function[13,14]. Notably, intestinal γδ17 T cells traffic to the meninges after ischemic brain injury[15], suggesting that γδ17 T cells populating peripheral tissues, including the gut, may also be involved in aberrant brain function under inflammatory conditions. Furthermore, γδ T cells and other types of T lymphocytes, such as regulatory T cells (T_{reg}) and IL-17-producing $CD4^+$ αβ T cells (T_H17 cells), can be regulated by commensal microorganisms in the gut and altered by ischemic stroke, maternal immune activation as well as chronic stress[15-17]. Surprisingly, despite the abundance of γδ T cells in the gut[8], the impact of chronic stress on intestinal γδ T cells and their roles in modulation of stress-induced behavioral consequences remain obscure.

Dectin-1 is a C-type lectin pattern-recognition receptor that is a crucial component of the innate immune system and widely expressed on myeloid cells as well as a subpopulation of T lymphocytes, including γδ17 T cells, and thereby potentially involved in immune surveillance, particularly at portals of pathogen entry such as the intestine[18,19]. Interestingly, colonic dectin-1 is involved in the microbiome alteration and immune/inflammatory responses in the colon of mice with colitis[20,21]. This suggests that dectin-1 may be involved in psychosocial stress responses via the T cell-mediated intestinal immune system.

In this study we investigate the effects of chronic social-defeat stress (CSDS) on intestinal microorganisms and the pathological roles of gut γδ T cells on behavioral vulnerability to CSDS. To gain translational insight into the psychopathology of depression, we examine microbiome signatures in patients with major depressive disorder (MDD). Furthermore, we explore the causal role of dectin-1 in the CSDS-induced pathophysiological processes and behavioral outcomes mediated by intestinal γδ T cells, and test pharmacological application targeting dectin-1 as a potential intervention for the prevention of stress-susceptible behavioral phenotypes.

Results

Altered microbial communities in mice with CSDS and patients with MDD

To investigate the relevance of gut-microbiota dysbiosis to stress-induced behavior, we examined the composition of the gut microbiota of a mouse model of CSDS[22]. Male C57BL/6 mice were subjected to 10 d of CSDS and then differentiated as stress-resilient or stress-susceptible according to their social-avoidance behavior in a three-chamber social interaction test[6,22] (Extended Data Fig. 1a,b). There was no difference in body-weight change between control, resilient and susceptible mice following CSDS (Extended Data Fig. 1c). Fecal samples were then collected for whole-genome shotgun metagenomic sequencing

of the gut microbiota, a method that provides higher resolution than *16S* ribosomal RNA gene amplicon sequencing (Fig. 1a). The intestinal microbial populations were less diverse in susceptible mice than the control and resilient mice (Shannon α-diversity index) and there was a distinct community overlap between the control mice and the resilient and susceptible mice (Jaccard β-diversity and Bray–Curtis indices; Fig. 1b,c and Extended Data Fig. 2a). At the genus level we detected altered compositions of the gut microbiota of resilient and susceptible mice compared with the controls, such as an expansion of *Parabacteroides* and a contraction of *Roseburia* (Extended Data Fig. 2b and Supplementary Table 1); this was consistent with previous studies of the gut microbiota of the mouse models of chronic stress paradigms using *16S* rRNA gene sequencing[23,24]. At the species level the relative abundance of *Lactobacillus johnsonii* was reduced in susceptible mice compared with control mice (Fig. 1d,e and Supplementary Table 1) and highly correlated with social-avoidance behavior (Fig. 1f). Moreover, at the strain level we identified several bacterial taxa that were altered in susceptible mice compared with the controls (Fig. 1g and Supplementary Table 1), including a lower abundance of *L. johnsonii* strains such as NCC 533 (La1), N6.2, pf01, DPC 6026 and ATCC 33200 (Fig. 1h-l). These results suggest that a reduced abundance of *L. johnsonii* may mediate CSDS-induced social-avoidance behavior.

To gain translational insight into the impact of microbiota alteration on human psychopathology, we also investigated the composition of the gut microbiota of patients with MDD and healthy controls (Supplementary Table 2). Our *16S* rRNA gene sequencing of stool samples indicated no differences in the diversity of intestinal microbial populations between these two groups (Chao1 α-diversity, Shannon α-diversity and phylogenetic diversity whole-tree indices; Supplementary Table 2). At the genus level, there was no statistically significant difference in composition of the gut microbiota of patients with MDD versus healthy controls after multiple-testing corrections (Fig. 1m). However, the relative abundance of *Lactobacillus* in patients with MDD was inversely correlated with scores in the Montgomery–Åsberg depression (MADRS), Hamilton depression (HAMD) and Hamilton anxiety (HAMA) rating scales (Fig. 1n-p). Multivariable regression analysis revealed no association between the relative abundance of *Lactobacillus* and several variables that are reportedly associated with microbiota alteration, including antidepressant dosage, sex, age and body mass index as well as the duration since the first episode of depression (Supplementary Table 3). Despite the differences between the intestinal microbial populations of mice and humans, these results indicate that the relative frequencies of *Lactobacillus* may influence stress vulnerability relevant to the psychopathology of depression.

Increased colonic and meningeal γδ17 T cells in susceptible mice

The impact of altered intestinal commensal microbiota on the gut immune system, particularly on T cell responses, has gained great attention in the pathophysiologies of inflammation-related diseases[21,25,26]. Given that *Lactobacillus* species are involved in T_{reg} cell differentiation in the colon[21] and the relative abundance of *L. johnsonii* is highly correlated with CSDS-induced social-avoidance behavior (Fig. 1e,f), we next explored the effects of CSDS on intestinal T cell populations (Fig. 2a). Flow cytometric analyses revealed a significant increase in the frequency and number of γδ and γδ17 T cells in the lamina

propria (LP) of the colon in susceptible mice compared with the controls, whereas no increase was seen in resilient mice (Fig. 2a); these striking cellular phenotypes in the susceptible mice were specific to the colon, as no differences in the frequencies of γδ and γδ17 T cells in the small intestine or spleen of susceptible and resilient mice was observed, although the frequency of γδ T cells in the small intestine of both resilient and susceptible mice was increased compared with the controls (Fig. 2b,c). Although the frequency of $CD3^+$ T cells in the small intestine (but not the colon and spleen) was increased in both resilient and susceptible mice compared with the controls, no statistically significant difference in the frequency of $CD4^+$ T, $CD8^+$ T, T_H17 and T_{reg} cells in the colon, small intestine or spleen was observed between the three groups of mice (Extended Data Fig. 3a-d). An increase in TCR-$\gamma\delta^+$ cells in the colon LP of susceptible mice was confirmed with immunohistochemistry assays (Fig. 2d). These results suggest that CSDS specifically increased the frequency of colonic γδ T cells as well as differentiation of γδ17 T cells in susceptible mice.

Given the involvement of meningeal γδ T cells in brain function and mouse behavior under steady-state conditions[13,14], we investigated whether CSDS affects the meningeal γδ T cell population by examining intact skull sections of mice after CSDS using immunohistochemistry. The γδ T cells were localized to the meninges, not the brain parenchyma, and the frequency of γδ T cells was increased in susceptible mice, not resilient mice, compared with the controls (Fig. 2e). Flow cytometry also revealed a specific increase in the frequency and number of γδ and γδ17 T cells in the meninges of susceptible mice (Fig. 2f). These results indicate that CSDS leads to the accumulation of γδ and γδ17 T cells in the meninges of susceptible mice.

To assess the sex effects of chronic stress on T cell populations, we used recently developed paradigms to mimic comparable stress effects in both sexes of C57BL/6 mice[27,28] (Extended Data Fig. 4a). Consistent with previous reports[27], the number and latency of CD-1 attacks was lower and slower across the 10-d CSDS period in female mice compared with males, and the estrous cycle had no effect on these behavioral phenotypes—that is, aggression and mounting (Extended Data Fig. 4b-f). Consistent with the social-avoidance behavior by susceptible female mice (Extended Data Fig. 4g), flow cytometry of meningeal T cell populations revealed an increase in the frequency of γδ and γδ17 T cells in susceptible female mice compared with both resilient and control female mice (Extended Data Fig. 4h). We did not observe any difference in the frequency of $CD3^+$ T, $CD4^+$ T, $CD8^+$ T, T_H17 or T_{reg} cells in the meninges between the three groups of female mice (Extended Data Fig. 4h).

Having shown that compared with control mice, susceptible mice exhibit a lower abundance of *L. johnsonii* (including *L. johnsonii* La1, which we found is the most prominent strain of *L. johnsonii* in mice gut microbiota; Fig. 1h), we next examined whether these microbiota changes are involved in CSDS-induced behavioral and γδ T cell phenotypes. Wild-type (WT) male mice were orally administered La1 or vehicle 10 d before and during the course of CSDS (Fig. 2g). We confirmed that La1 was severely decreased by CSDS and increased by the oral administration of La1 (Extended Data Fig. 5). We observed that La1 administration suppressed CSDS-induced elevation in the frequency of both γδ and γδ17 T cells in the colon and also promoted resilience to social-avoidance behavior (Fig.

2h,i). These results suggest that the reduced abundance of La1 contributes to both the CSDS-induced increased frequency of colonic γδ T cells and γδ17 T cell differentiation as well as social-avoidance behavior.

Inhibition of peripheral γδ T cells blocks social avoidance

Following a stroke, gut dysbiosis affects intestinal γδ17 T cell differentiation and trafficking to the meninges via intestinal T_{reg} cell-mediated mechanisms[15]. We thus reasoned that CSDS-induced colonic γδ17 T cell differentiation is causally linked to an elevation of meningeal γδ17 T cells and the resultant social-avoidance behavior. To test this hypothesis, we first examined the effect of CSDS on the repertoire of meningeal γδ T cells. γδ T cells are categorized based on the type of γ chain variable region (Vγ) of the T cell receptor[29,30]. $V\gamma6^+$ γδ T cells are the major population of γδ T cells in the meninges, whereas $V\gamma7^+$ γδ T cells are more commonly found in the gut[13,14,29]. Flow cytometry analysis revealed that meningeal γδ T cells in control and resilient mice indeed mainly consist of $V\gamma6^+$ γδ T cells (Fig. 3a). Interestingly, we found that susceptible mice had altered compositions of meningeal γδ T cell populations characterized by a decreased frequency of $V\gamma6^+$ γδ T cells and an increased frequency of $V\gamma7^+$ γδ T cells (Fig. 3a). These results further support the idea that peripheral γδ T cells may be involved in the CSDS-induced increased frequency of γδ T cells in the meninges.

We then examined the impact of γδ T cell inhibition on CSDS-induced phenotypes by intraperitoneally (i.p.) injecting mice with an antibody to TCR γ and δ (anti-TCR-γδ; UC7-13D5), which internalizes TCR-γδ[13], or its isotype control (IgG; Fig. 3b). The percentages of γδ T cells in the spleen were reduced on days 3, 7 and 12 following i.p. injection with either 50 or 250 μg anti-TCR-γδ (Extended Data Fig. 6a,b). Importantly, we did not observe any change in the frequency of meningeal γδ T cells (Extended Data Fig. 6c). These results suggested that i.p. injection with anti-TCR-γδ, at a dosage of 50 μg, 1 d before the start of CSDS for 10 d allows for suppression of the peripheral γδ T cell population under chronic stress conditions (Fig. 3b). In fact, treatment with anti-TCR-γδ suppressed the frequency of colonic γδ T cells both under non-CSDS and CSDS conditions (Fig. 3c). Intriguingly, despite the same frequency of meningeal γδ T cells in non-CSDS control mice receiving anti-TCR-γδ and those receiving IgG, the increased frequency of meningeal γδ T cells in CSDS mice was suppressed by anti-TCR-γδ (Fig. 3d). This finding implies that the CSDS-induced increased frequency of meningeal γδ T cells is attributed to peripheral γδ T cells trafficking to the meninges.

We next examined the effect of anti-TCR-γδ treatment on the CSDS-induced behaviors. Neither CSDS nor treatment with anti-TCR-γδ affected locomotor activity in the open field test (Extended Data Fig. 6d). Furthermore, i.p. injection of anti-TCR-γδ did not affect anxiety-like behaviors induced by CSDS in the elevated plus maze test (Extended Data Fig. 6e), although intra-cisterna magna injection of anti-TCR-γδ reportedly had an anxiolytic effect under steady-state conditions[13]. Consistent with its inhibition of the increase in colonic and meningeal γδ T cell populations, the anti-TCR-γδ treatment promoted resilience to the social avoidance induced by CSDS in a three-chamber social interaction test (Fig. 3e). To further assess the role of γδ T cells in stress-induced psychopathology,

we performed a sucrose preference test to characterize loss of consummatory pleasure, a potential component of anhedonia, by measuring taste reward[22]. To examine whether the CSDS-induced reduction in consummatory pleasure is affected by peripheral γδ T cell inhibition, we subjected anti-TCR-γδ- and IgG-treated mice to an 8-d sucrose preference test following the social interaction test. There were no differences in total fluid consumption between the anti-TCR-γδ- and IgG-treated control and CSDS mice (Extended Data Fig. 6f). The CSDS mice exhibited reduced preference for the sucrose solution compared with the controls, a behavior phenotype that was inhibited by anti-TCR-γδ treatment (Extended Data Fig. 6g). These results suggest that peripheral γδ T cells contribute to CSDS-induced social avoidance and reduced consummatory pleasure.

Peripheral γδ17 T cells are required for CSDS-induced behaviors

Given the increased frequency of γδ17 T cells in the colon of susceptible mice compared with resilient and control mice (Fig. 2a), we next examined whether peripheral γδ17 T cells are required for the social-avoidance behavior of the mice exposed to CSDS. To this end, mice deficient in γδ T cells (TCRd-KO) and their WT littermates were subjected to CSDS, followed by a social interaction test (Fig. 4a). Consistent with the beneficial effect of peripheral anti-TCR-γδ treatment on CSDS-induced social avoidance, TCRd-KO mice did not show abnormal sociability in response to CSDS (Extended Data Fig. 6h). To elucidate the specific role of peripheral γδ17 T cell differentiation in CSDS-induced behaviors, we isolated γδ T cells from mice carrying the gene encoding green fluorescent protein (GFP) at the endogenous *Il17a* locus (IL-17 GFP mice). TCRd-KO mice were adoptively transferred with isolated γδ T cells or vehicle 1 d before and 5 d after the start of CSDS by retro-orbital intravenous (i.v.) injection (Fig. 4a). Whereas CSDS resulted in no social-avoidance behavior in vehicle-injected TCRd-KO mice, γδ T cell adoption impaired the sociability of the TCRd-KO mice exposed to CSDS (Fig. 4b). Immunohistochemical staining revealed engraftment of transferred GFP^+ γδ17 T cells into the colon and meninges of the TCRd-KO mice; furthermore, this engraftment was increased by CSDS, supporting the essential role of γδ17 T cells in these pathophysiological processes (Fig. 4c,d). Flow cytometry analysis demonstrated an increased frequency of both transferred γδ and γδ17 T cells in the meninges of the TCRd-KO mice subjected to CSDS (Fig. 4e). Interestingly, we found it difficult to detect a clear γδ T cell population in the meninges, suggesting modest migration of the adoptively transferred γδ T cell population into the meninges. However, we were able to detect adoptively transferred γδ17 T cells more easily using an antibody to GFP and we identified a clear GFP^+ γδ17 T cell population in the meninges. Together, these findings indicate that chronic stress increases colonic γδ T cells and γδ17 T cell differentiation, which contribute to the elevation in meningeal γδ17 T cells, consequently leading to stress-susceptible behavioral phenotypes.

Dectin-1 mediates colonic γδ17 T cell differentiation and behavioral deficits

We next sought to gain an insight into the molecular mechanisms underlying the CSDS-induced pathophysiological processes and behavioral outcomes mediated by intestinal γδ17 T cells. As described earlier, colonic dectin-1—a crucial component of the innate immune system[18,19]—regulates intestinal inflammation via commensal *Lactobacillus*-mediated modulation of T cell differentiation[21]. Dectin-1 recognizes β-glucan polysaccharides

(including 1,3-β-D-glucan) derived from fungal cell walls[31-33], the degradation of which is mediated by *L. johnsonii* in the gut[34]. Our results demonstrate that the reduced frequency of intestinal *L. johnsonii* contributes to the CSDS-induced expansion of colonic γδ T cells and γδ17 T cell differentiation as well as to social-avoidance behavior (Fig. 1e-l and Fig. 2h,i). Thus, we investigated whether dectin-1 mediates CSDS-induced alteration of colonic γδ T cell populations and social behavioral abnormalities. We found that dectin-1 was expressed in colonic γδ T cells and the frequency of dectin-1$^+$ γδ T cells was elevated in susceptible mice compared with resilient and control mice (Fig. 5a). Although dectin-1 was also expressed in CD3$^+$, CD4$^+$ and CD8$^+$ T cells, the frequency of the dectin-1$^+$ cell population was similar in the three groups of mice (Extended Data Fig. 7), suggesting that CSDS-induced dectin-1 elevation is γδ T cell-specific in colonic T cell populations.

We therefore hypothesized that CSDS-induced upregulation of dectin-1 signaling in colonic γδ T cells leads to an increase in γδ17 T cell differentiation and consequent social behavioral abnormalities. To test this hypothesis, we compared the impact of CSDS on the colonic T cell populations and social behavior of mice with a genetic deletion of dectin-1 (*Clec7a*$^{-/-}$) with their WT littermates. Although CSDS increased the frequency of γδ, γδ17 and CD8$^+$ T cells in the colon of the WT mice, the frequency of these three cell populations was not elevated in the colon of the *Clec7a*$^{-/-}$ mice after CSDS (Fig. 5b and Extended Data Fig. 8c). The frequency of CD3$^+$ T, CD4$^+$ T, T_H17 and T_{reg} cells in the colon of *Clec7a*$^{-/-}$ mice remained unchanged following CSDS (Extended Data Fig. 8a,b,d,e). Consistent with these data, *Clec7a*$^{-/-}$ mice showed no abnormalities in sociability and CSDS did not induce social-avoidance behavior in *Clec7a*$^{-/-}$ mice (Fig. 5c). Although no differences in total fluid consumption were observed between *Clec7a*$^{-/-}$ mice and controls during a sucrose preference test, CSDS decreased the sucrose preference of control mice but not *Clec7a*$^{-/-}$ mice (Extended Data Fig. 8f,g).

We further examined whether dectin-1 expression on γδ T cells is required for the social-avoidance behavior observed in the CSDS model. We isolated γδ T cells from *Clec7a*$^{-/-}$ mice and their WT littermates, and adoptively transferred the cells into TCRd-KO mice by i.v. retro-orbital injection 1 d before and 5 d after the start of CSDS. After CSDS the mice were subjected to a social interaction test, followed by tissue harvesting for subsequent flow cytometry analysis (Extended Data Fig. 8h). We found that the frequency of both colonic γδ and γδ17 T cells in TCRd-KO mice with dectin-1 knockout (dectin-1-KO; *Clec7a*$^{-/-}$) γδ T cell adoption was significantly lower than those in the TCRd-KO mice with WT γδ T cell adoption (Fig. 5d). We also observed that TCRd-KO mice with WT γδ T cell adoption, but not those with dectin-1-KO γδ T cell adoption, exhibited CSDS-induced social-avoidance behavior (Fig. 5e). These results suggest that dectin-1 expressed on γδ T cells contributes to CSDS-induced colonic γδ T cell expansion and γδ17 T cell differentiation as well as social-avoidance behavior.

We also wanted to explore the effect of pharmacological modulation of dectin-1 on the CSDS-induced elevation of the colonic γδ T cell population and behavioral phenotypes. Wild-type mice were orally administered vehicle or pachyman—a 1,3-β-D-glucan extracted from the saprophytic fungus *Poria cocos* that is used for complementary treatment of depression[35]—during the course of CSDS (Extended Data Fig. 8i). Flow cytometry revealed

that treatment with pachyman inhibited CSDS-induced elevation of the frequency of γδ, γδ17 and $CD8^+$ T cells in the colon but had no effect on these cell populations under non-CSDS conditions (Fig. 5f and Extended Data Fig. 8l). The frequency of colonic $CD3^+$ T, $CD4^+$ T, T_H17 and T_{reg} cells did not differ between groups (Extended Data Fig. 8j,k,m,n). As observed in the social interaction test, treatment with pachyman reversed social-avoidance behaviors induced by CSDS but had no effect on the sociability of control mice that were not exposed to CSDS (Fig. 5g). Although no difference in total fluid consumption was observed between groups in the sucrose preference test, pachyman treatment restored sucrose consumption in the CSDS group and had no effect on the controls (Extended Data Fig. 8o,p). These results suggest that dectin-1 mediates CSDS-induced elevation of colonic γδ T cell populations and γδ17 T cell differentiation as well as the resultant social-avoidance and reduced consumption behaviors.

Intestinal γδ T cell differentiation is independent of IL-1β in myeloid cells

Previous studies showed that γδ T cell expansion and γδ17 T cell differentiation is mediated by IL-1β and IL-23 derived from myeloid cells[9,36]. We therefore examined whether CSDS affects colonic myeloid cell populations and their IL-1β and IL-23 production as well as whether dectin-1 is involved in these cellular effects. Flow cytometry analysis revealed that the frequency of monocytes and macrophages ($CD45^+Ly6C^+CD11b^+CX3CR1^+$ and $CD45^+Ly6C^-CD11b^+CX3CR1^+MHCII^+$, respectively), but not dendritic cells ($CD45^+CD11c^+CX3CR1^-MHCII^+$), was significantly increased in susceptible mice (Fig. 6a,b). The frequency of dectin-1^+ monocytes and macrophages was decreased in resilient and susceptible mice, whereas CSDS did not affect the frequency of dectin-1^+ dendritic cells (Fig. 6c). The frequency of colonic IL-1β-producing monocytes ($CD45^+Ly6C^+CD11b^+CX3CR1^+MHCII^+$) in both resilient and susceptible mice as well as the frequency of colonic IL-23-producing monocytes in resilient mice was increased by CSDS (Fig. 6d,e). Critically, genetic deletion of dectin-1 had no effect on CSDS-induced elevation of the frequency of IL-$1β^+$ producing monocytes (Fig. 6f), suggesting that IL-1β production does not directly mediate the inhibitory effect of dectin-1 deletion on CSDS-induced increased colonic γδ T cell populations and γδ17 T cell differentiation. Consistent with these data, colonic γδ T cells were co-stained with orally administered fluorescein dichlorotriazine (DTAF)-labeled pachyman, and these histochemical phenotypes were reduced by genetic deletion of dectin-1 (Fig. 6g). These results indicate that dectin-1 expressed in colonic γδ T cells mediates the effect of orally administered pachyman on CSDS-induced colonic γδ T cell expansion and γδ17 T cell differentiation.

Discussion

We demonstrate an aberrant gut immune system that interacts with intestinal flora, contributing to stress-induced behavioral outcomes relevant to depression. In particular, our study shows that colonic γδ17 T cell differentiation and meningeal accumulation of γδ17 T cells are cellular mechanisms underlying stress-susceptible behavioral phenotypes. Despite diverse evidence from gut-microbiota profiling in rodent models of stress, several studies have demonstrated that chronic stress reduces the relative abundance of *Lactobacillus* in the

gut[37-39]. Specific commensal intestinal microbiota, such as *Lactobacillus* and *Clostridium* species, induce expansion and differentiation of intestinal T_{reg} cells, thus protecting the host immune system[21,26,40]. Intestinal T_{reg} cells suppress γδ T cell expansion and γδ17 T cell differentiation to maintain gut immune homeostasis and the anti-inflammatory environment[15,41]. Our results imply a role for *L. johnsonii* in the stress-induced colonic γδ T cell expansion and γδ17 T cell differentiation that produces stress-susceptible behavioral outcomes. Our observation of a negative correlation between the relative abundance of *Lactobacillus* and depressive symptoms in patients with MDD suggests that the CSDS-induced alterations in *Lactobacillus* species that contribute to social-avoidance behavior may be relevant to human psychopathology.

Although the CSDS model that we used in this study is a well-established approach to examine the impact of stress in male mice[42], we have also shown that the newly developed paradigm for CSDS in female mice[27,28] induced social-avoidance behavior and γδ T cell phenotypes in a small cohort of female mice. Considering sex differences in the prevalence of depression and in immune responses[43,44], it is important for future studies to examine sex effects on dectin-1 expression in the γδ T cell-mediated stress-response mechanism.

Growing evidence highlights the underappreciated roles of the contribution of T lymphocytes to behavioral phenotypes under chronic stress[45,46]. γδ T cells are a subgroup of T lymphocytes that are enriched in the peripheral tissues, including the intestine, and play unique roles in not only adaptive immunity but also the innate-like response and inflammatory pathophysiology[8,30,47]. In addition to the immune surveillance activities of γδ T cells in the mucosa, recent findings reveal the crucial contribution of the meningeal-resident γδ17 T cells to the control of brain function and behaviors. Under steady-state conditions the meningeal-resident γδ17 T cells release IL-17a and regulate anxiety-like behavior via neuronal IL-17a receptor signaling[13]. Furthermore, the meningeal-resident $V\gamma6^+$ γδ T cell subset produces IL-17 and regulates short-term memory[14]. Interestingly, however, γδ T cells enriched in the gut preferentially traffic and accumulate in the meninges after ischemic brain injury, a feature that can be suppressed by gut-microbiota modulation[15]. We have now demonstrated that CSDS elevates colonic γδ17 T cell differentiation and the meningeal accumulation of γδ17 T cells associated with stress-susceptible behavioral phenotypes. Given that peripheral manipulation of γδ T cells normalizes these γδ17 T cell phenotypes and behavioral outcomes, intestinal γδ T cells migrating into the meninges may also be involved in the pathophysiological processes affecting brain function in an inflammatory environment, such as under chronic stress conditions.

Our results demonstrate that CSDS-induced colonic γδ17 T cell differentiation and meningeal accumulation of γδ17 T cells is mediated by dectin-1, an innate immune receptor critical for recognizing β-glucan polysaccharides, a component of fungal cell walls[18,31,33]. Previous studies show that dectin-1 directs the differentiation of multiple T cell subtypes—for example, dectin-1 expressed on macrophages is involved in the differentiation of $CD4^+$ and $CD8^+$ T cells into immunogenic or tolerogenic phenotypes[48]. Dectin-1 also regulates gut immunity homeostasis by controlling T_{reg} cell differentiation in the intestine through modification of microbiota including *Lactobacillus* species[21]. Surprisingly, although dectin-1 is predominantly expressed on the surface of myeloid cells[18], CSDS

induces elevation of dectin-1 expression specifically on γδ T cells but not on monocyte/macrophages, dendritic cells or other types of T cells of susceptible mice. Our results also demonstrate that dectin-1 expressed on γδ T cells mediates CSDS-induced expansion of colonic γδ T cells and γδ17 T cell differentiation as well as the resultant social-avoidance behaviors. Although further studies are required to examine the complex roles of dectin-1 in other cell types along the gut–brain axis under stress conditions, our results provide strong evidence of the pathological role of dectin-1 expressed on γδ T cells, as it directly contributes to colonic γδ T cell expansion and γδ17 T cell differentiation, as well as to the behavioral outcomes induced by CSDS.

Finally, our study provides proof-of-principle that pharmacological intervention targeting dectin-1 may be useful for the development of treatments to prevent stress-induced behavioral abnormalities. Dectin-1 inhibition suppresses intestinal inflammation by T_{reg} cell expansion in mouse models of colitis; furthermore, dectin-1 is activated by the ligands in the intestine and modulates T cell differentiation[21]. In the context of dectin-1 impacting T cell function, we reveal that the dectin-1 ligand pachyman inhibits CSDS-induced colonic γδ17 T cell differentiation and meningeal accumulation of γδ17 T cells, alleviating the resultant social avoidance and reduced consummatory pleasure. Interestingly, recent studies in a mouse model of inflammatory bowel disease suggest that β-glucans control the commensal *Lactobacillus* in the colon via dectin-1 signaling, and *L. johnsonii* modulates intestinal inflammation and eliminates fungi via its antifungal enzyme activities[20,34]. Considering the high prevalence of depression in patients with inflammatory bowel disease[49,50], the crosstalk between *L. johnsonii*–fungi imbalance and dectin-1 signaling is underscored as a pathological process impacting intestinal T cell function, in which disturbance is involved in stress-induced behavioral phenotypes.

In summary, our findings highlight unrecognized γδ T cell-mediated gut immunity mechanisms impacting psychosocial stress responses. With the growing interest in the pathological implication of IL-17 and T lymphocytes in depression, there is a clear need to further investigate the precise roles of γδ T cell in stress susceptibility. Elucidating the precise molecular mechanisms underpinning dectin-1-mediated colonic γδ17 T cell differentiation may pave the way for novel treatment and prevention of stress-related psychiatric disorders such as depression.

Methods

Mice

C57BL/6J *Il17a–eGFP* (C57BL/6-Il17a^{tm1Bcgen}/J) and *Tcrd*$^{-/-}$ (B6.129P2-Tcrd^{tm1Mom}/J) mice were purchased from Jackson Laboratories. Retired CD-1 breeder adults were purchased from Charles River Laboratory. *Clec7a*$^{-/-}$ mice were a gift from R. Giger at the University of Michigan, T. Hohl at the Sloan Kettering Institute and Y. Iwakura at the Tokyo University of Science. Genetically modified lines were bred in our facility. The animals that were purchased from Jackson Laboratories were maintained for at least 1 week to allow for habituation before experimentation. When both male and female mice were used, the animals were sex- and age-matched in each experiment. The mice were housed under standard 12 h light–dark cycle conditions in rooms maintained at 21 °C with

30–70% humidity. All animal procedures were approved by the Institutional Animal Care and Use Committee of Johns Hopkins University School of Medicine and adhered to ethical consideration in animal research.

Human study participants

Between June 2017 and September 2020, 40 patients with depression and 34 healthy control individuals ≥20 yr of age were recruited at Showa University Karasuyama Hospital, Keio University Hospital and Komagino Hospital in Tokyo. Of these, fecal samples from 32 patients (17 females; age, 56.2 ± 19.1 yr) and 34 control individuals (18 females; age, 56.1 ± 12.3 yr) who had at least one clinical measurement were included in the statistical analysis. The inclusion criteria for patient recruitment were: (1) meets the diagnostic and statistical manual of mental disorders, 5th edition, criteria for MDD; (2) ≥20 yr old and (3) able to give informed consent. The exclusion criteria were individuals that (1) had any organic gastrointestinal disorders, (2) took antibiotic medication at any time during the study or (3) whose participation in the trial could worsen their psychiatric symptoms. The clinical trial was approved by the Ethical Committee of Showa University Karasuyama Hospital and Keio University School of Medicine in accordance with the ethical guidelines for medical and health research involving human participants composed by the Japan Ministry of Health, Labor and Welfare. The trial was also registered with the UMIN Clinical Trials Registry (UMIN000021833). This was a multicenter prospective observational study conducted at Showa University Karasuyama Hospital, Keio University Hospital and Komagino Hospital in Tokyo. All patients were informed about the purposes and procedures of the study with a thorough explanation and provided written consent. Fecal samples were collected and psychiatric assessments were performed during a naturalistic treatment course. The fecal samples were frozen immediately following collection and stored at −80 °C until analysis.

Study procedure

For inpatients, fresh fecal samplings and psychiatric assessments were performed during the hospitalization. Baseline assessments were conducted within 10 d of admission, midterm assessments were done between 14 and 20 d after admission, and endpoint assessments were done 21 d after admission and before discharge. A period of at least 1 week was designated as an evaluation interval. For outpatients, fresh fecal samplings and psychiatric assessments were performed at outpatient visits and fecal samples were stored at −80 °C until the analysis. Comprehensive psychiatric assessments comprising psychiatric history, and HAMD[51], MADRS[52] and HAMA[53] scales were administered by trained psychiatrists and psychologists when the fecal samplings were performed. The Pittsburgh sleep quality index[54] was assessed at baseline. In this study we only used the data from the baseline assessment.

16S rRNA gene sequencing and analysis of human samples

Fecal samples were immediately frozen after collection and transported to either the Showa University Karasuyama Hospital or Keio University Hospital within 48 h. They were kept in a freezer at −80 °C for further analyses. The *16S* rRNA gene was analyzed as previously described with some modifications[55]. First, the fecal samples were lyophilized for approximately 12–18 h using a VD-800R lyophilizer (TAITEC). Each freeze-dried

fecal sample was combined with four 3.0-mm zirconia beads and subjected to vigorous shaking (1,500 r.p.m. for 10 min) using a Shake Master (Biomedical Science). Second, approximately 10 mg of each fecal sample was combined with approximately 100 mg of 0.1-mm zirconia/silica beads, 300 μl DNA extraction buffer (TE containing 1% (wt/vol) SDS) and 300 μl of phenol–chloroform–isoamyl alcohol (25:24:1), and subjected to vigorous shaking (1,500 r.p.m. for 5 min) using a Shake Master. The resulting emulsion was subjected to centrifugation at 17,800*g* for 10 min at room temperature. RNA was removed from the sample by RNase A treatment of the bacterial genomic DNA purified from the aqueous phase. The resulting DNA sample was then further purified by another round of phenol–chloroform–isoamyl alcohol treatment and ethanol precipitation by GENE PREP STAR PI-480 (Kurabo Industries Ltd.). The V1–V2 hypervariable region of 16S rRNA-encoding genes were amplified by PCR using a bacterial universal primer set[40,56]. The amplicons were analyzed using a MiSeq sequencer (Illumina) with some modifications, as previously indicated[55]. Filter-passed reads were processed using Quantitative Insights into Microbial Ecology 2 (October 2019)[57]. Denoising and trimming of sequences were processed using DADA2. To remove the primer sequences, 20 and 19 base pair (bp) reads were trimmed from the 5′ ends of the forward and reverse reads, respectively; 280- and 210-bp read lengths from the 5′ ends were used for further steps. Taxonomy was assigned using the SILVA132 (refs. [58,59]) database using the Naive Bayesian Classifier algorithm. The α-diversity of gut microbiota was analyzed using Chao1, Shannon and phylogenetic diversity whole-tree indices.

CSDS

Male mice were subjected to CSDS[6,22,42]. Briefly, a singly caged mouse (test mouse) was exposed to a screened novel aggressive CD-1 mouse (aggressor mouse) for 10 min each day for ten consecutive days. Following 10 min of contact, the test mouse and aggressor mouse were separated by a transparent and porous Plexiglas divider within the home cage of the CD-1 aggressor. The test mouse was thus exposed to chronic stress in the form of a threat for 24 h following each exposure. Nonstressed control mice were housed in equivalent cages but with members of the same strain. The mice that were placed with the controls were also changed daily. Female mice were subjected to CSDS as reported, with slight modifications[27,28]. Briefly, as a pair, a female (test) and male mouse were placed into the home cage of a screened novel aggressive CD-1 mouse (aggressor) for 10 min every day for ten consecutive days. In addition, urine collected from a male CD-1 mouse unfamiliar to the resident CD-1 mouse was applied to the female test mouse at the base of the tail (20 μl) and on the vaginal orifice (20 μl) immediately before being placed in the home cage of the aggressor mouse. Each female mouse was paired with the urine of a particular CD-1 mouse throughout the entire course of social defeat. Following 10 min of contact, the female test mouse and the CD-1 aggressor mouse were separated by a transparent and porous Plexiglas divider within the home cage of the CD-1 aggressor. The female test mouse was thus exposed to chronic stress in the form of a threat for 24 h after each exposure. As a control, a separate group of female and male mice were concurrently placed in a standard cage and allowed to interact without the presence of a CD-1 mouse for 10 min for 10 d. After 10 min of contact, the female control mouse was housed on one side of a divider with the male mouse on the other for 24 h until the next interaction session. The male mice that

interacted with the female controls were changed daily. These female control mice also had male urine applied to them. Urine collection from CD-1 mice and the estrous cycle state assessment of the female test mouse were performed as described elsewhere[27,28].

La1 treatment

The La1 preparation and administration were performed using previously published methods[60,61], with minor modifications. Briefly, La1 was cultured for 20 h at 37 °C in 50 ml anaerobic BD Difco lactobacilli MRS broth (Fisher Scientific) supplemented with 1% glucose and 0.05% cysteine[60,62]. Heterotrophic plate counting and optical density at 600 nm were performed to determine the bacterial concentrations. The bacterial cells were collected by centrifugation (10,000*g* for 5 min at 4 °C) and suspended in PBS pH 7.0. The concentration of the suspension was set to 1×10^{10} colony-forming units ml^{-1} and a suspension containing 1×10^{9} La1 cells was orally administered from 10 d before and during the course of CSDS. The vehicle-treated groups were orally administered with PBS during the same period as the La1 groups.

Pachyman treatment

One hour before social defeat, the test mice were orally treated with 200 mg kg^{-1} pachyman (>98% purity, Megazyme) or vehicle every day for 10 d. This dosage was previously reported to have an effect on immune function in mouse models[63]. For all manipulations, care was taken to handle the animals gently to minimize stress. During the pachyman treatment, all of the mice were housed following the CSDS protocol and their social-avoidance behavior was tested 24 h following the treatment.

Three-chamber social interaction test

Social-avoidance behaviors were tested using a previously published protocol[6,22]. Briefly, the test mice were placed in a three-chamber apparatus (40 cm width × 20 cm height × 26 cm depth) in which both side chambers contained a plastic cage in the corner. The trial consisted of three sessions, beginning first with 10 min habituation in the center chamber, followed by a second 10-min session during which the test mouse was allowed to freely explore all three chambers. Before the third session, the test mouse was gently guided to and confined in the center chamber, during which time a stranger mouse of the same strain was placed in one of the two peripheral plastic cages and an inanimate object was placed in the other. In the third session, the test mouse was allowed to freely explore all three chambers for 10 min. The behavior of the mice was monitored via video, and the trajectory of mouse ambulation was automatically determined and recorded using the video tracking system TopScan 3.0 (CleverSys). The apparatus was cleaned with a solution of 70% ethanol in water to remove olfactory cues following each trial and all of the behavioral tests were conducted in the dark. To separate the stress-susceptible and stress-resilient subpopulations, the times spent by the test mouse in each chamber and sniffing each object were recorded and a social interaction ratio (time in chamber with the stranger or time in chamber with the inanimate object) of 1.0 was set as the cutoff. Mice with scores <1.0 were considered stress-susceptible and those with scores ≥1.0 were considered stress-resilient. The heatmaps were generated using Ethovision XT 11.0 (Noldus).

Open field test

The open field test was performed using our published protocol, with minor modifications[64,65]. Briefly, a mouse was gently placed in the center of an open field cage and left to explore the open field for 30 min. Locomotor activity was measured using a Photobeam Activity System (PAS–Open Field, San Diego Instruments). The PAS system consisted of two vertically stacked frames, each containing infrared lasers arranged in a 16 × 16 grid, which detected mouse movements such as ambulation and rearing. Single-beam breaks were automatically recorded as ‘counts’ and the PAS system automatically started recording counts once the mouse started moving. The total counts were recorded and used for analyses. The open field box and surrounding photobeam apparatus were housed in a ventilated cabinet.

Elevated plus maze test

The elevated plus maze consisted of a plus-shaped apparatus with two opposing open arms (30 cm × 5 cm × 0.5 cm) and two opposing enclosed arms (30 cm × 5 cm × 15 cm) connected by a central platform (5 cm × 5 cm), elevated 61 cm above the floor. The test was performed in a dimly lit experiment room in which the mice were acclimatized for at least 30 min before testing. The times that were spent in the open arms and the enclosed arms were recorded over a 5 min test period using the TopScan 3.0 video tracking system (CleverSys) and the time spent in the open arms was used for analyses.

Sucrose preference test

The sucrose preference test was performed as previously reported[22]. Briefly, mice were singly caged before the test. On day 1 their normal water bottles were replaced with two 50 ml tubes (bottle ‘A’ and bottle ‘B’) fitted with bottle stoppers containing two-balled sipper tubes. Before the sucrose preference test, the mice were habituated to a 1.5% sucrose solution for 4 d as follows: on days 1 and 2 both bottles were filled with normal drinking water and on days 3 and 4 both bottles were filled with 1.5% sucrose dissolved in drinking water. Following the habituation period, the sucrose preference test was conducted for 4 d between days 5 and 8. On the test days bottle A contained 1.5% sucrose solution and bottle B contained drinking water. The positions of bottles A and B were switched daily to avoid a side bias and the fluid consumed from each bottle was measured daily. Sucrose preference was calculated for every mouse each day as 100% × (vol A ÷ (vol A + vol B)) and the total fluid consumption was calculated as vol A + vol B.

Mouse fecal sample collection and DNA extraction

Fresh stool pellets were collected and stored at −80 °C. The frozen stool samples (approximately 100 mg) were placed in QIAGEN PowerBead tubes and vortexed on a QIAGEN PowerLyzer homogenizer at 1,500 r.p.m. for 90 s, followed by a 90-s pause and then 90 s at 1,500 r.p.m. DNA was extracted using the PowerSoil pro kit (QIAGEN) according to the manufacturer’s instructions.

Metagenomic sequencing and analysis of mouse stool samples

DNA libraries were prepared using a Nextera XT library preparation kit (Illumina) with a modified protocol. Library quantity was assessed using a Qubit 4.0 fluorometer (ThermoFisher). The completed library was sequenced on an Illumina HiSeq 4000 system, 2 × 150 bp, following the Illumina-recommended procedures. Unassembled sequencing reads were directly analyzed using the CosmosID bioinformatics platform (CosmosID Inc.) for multi-kingdom microbiome analysis, profiling of antibiotic resistance and virulence genes, and quantification of the relative abundance of an organism, as described elsewhere[66-69]. Briefly, the system uses curated genome databases in addition to a high-performance data-mining algorithm that are able to rapidly disambiguate hundreds of millions of metagenomic sequence reads into the discrete microorganisms engendering those particular sequences.

Quantitative real time PCR

Bacterial DNA was isolated from the colonic fecal samples using a Quick-DNA fecal/soil microbe miniprep kit (cat no. D6010, Zymo Research) and subjected to quantification of La1 using quantitative real time PCR. Briefly, amplifications were carried out on an Applied Biosystems QuantStudio 5 system using the following conditions: 2 min at 95 °C, followed by 50 cycles of 5 s at 95 °C and 30 s at 60 °C. The amplification mixture with a final volume of 20 μl consisted of 10 μl PowerUp SYBR Green master mix (cat no. A25741, Applied Biosystems), 6.8 μl nuclease-free water, 2 μl template DNA and 0.6 μl of each forward and reverse primer. The following primers were used for the amplification of the La1 gene: Forward, 5′-TGCGCTCTAAAGTCTC ACAAGT-3′ and Reverse, 5′-GTTCGGCTCACTTTAATTGGTTTAC-3′. Universal Eubacteria (Forward, 5′-ACTCCTACGGGAGGCAGCAGT-3′ and Reverse, 5′-GTATTACCGCGGCTGCTGGCAC-3′) was used as a reference gene to normalize the expression data using the ddC_t method.

Cell isolation from spleen

Mice were anesthetized with isoflurane and transcardially perfused with 20 ml cold PBS. After perfusion the spleen was collected and minced into small pieces with a razor. The cut tissue was placed on a 70-μm cell strainer that had been pre-wet with 1 ml PBS and homogenized with the end of a 1-ml syringe plunger. Cells were then eluted from the strainer with 10 ml PBS. After centrifugation at 300*g* for 10 min, the cell pellet was resuspended in 5 ml ACK lysing buffer (Quality Biological) and incubated for 5 min at room temperature. The cell suspensions were then washed with 30 ml PBS and incubated for 10 min at 4 °C. The cell suspensions were filtered through a 70-μm cell strainer, centrifuged at 300*g* for 10 min and subsequently stained for flow cytometry analysis.

Isolation of intestinal LP mononuclear cells

Isolation of intestinal LP mononuclear cells was performed according to a previously reported method[15]. Briefly, mice were anesthetized with isoflurane and transcardially perfused with 20 ml cold PBS. The small intestine and colon of the mice were removed and isolated, followed by excision of Peyer's patches. The intestines were cleansed of mesenteric fat and other intestinal contents. Next, the intestines were opened lengthwise and washed

with PBS. They were then cut into pieces of 0.5–1 cm, which were washed with 20 ml of HBSS containing 10 mM HEPES (pH 7.2), 8% fetal bovine serum, 4 mM EDTA and 0.5 mM dithiothreitol for 20 min in a shaking incubator set at 250 r.p.m. and 37 °C. After three rounds of this wash, the tissue pieces were rinsed with Ca^{2+}-Mg^{2+}-PBS to remove the EDTA, followed by thorough mincing and subsequent placement into a digestion buffer containing 5 ml HBSS with 10 mM HEPES (pH 7.2), 5% fetal bovine serum and 0.2 mg ml^{-1} collagenase D (Millipore Sigma). The tissues were digested for 20 min with constant agitation (250 r.p.m.) at 37 °C before being vigorously vortexed for 20 s. The resulting cell suspension containing LP mononuclear cells was passed through a 70-μm strainer, assisted by gentle homogenization with the end of a 1-ml syringe plunger, and washed with 10 ml PBS. The LP mononuclear cell suspensions were collected via centrifugation at 500*g* for 10 min at 4 °C. The cell pellets were resuspended in 8 ml of 44% Percoll (GE Healthcare) and then overlaid with 5 ml of 67% Percoll. The gradients were centrifuged at 500*g* for 20 min at 4 °C, after which the cells at the interface were collected and washed with 10 ml PBS. The resulting cell suspension was centrifuged at 1,000*g* for 10 min at 4 °C to collect cells for flow cytometry analysis.

Meningeal cell isolation

Cell collection from the meninges was performed according to a previously described protocol[15]. Mice were anesthetized with isoflurane and transcardially perfused with 20 ml cold PBS. The upper portion of the cranium was separated from the brain and the meninges were isolated by careful peeling from the skull bones using surgical forceps under a dissection microscope. The meninges were placed on the surface of a 70-μm cell strainer pre-moistened with 1 ml PBS. The tissue was gently homogenized through the strainer with the end of a 1-ml syringe plunger, washed with 5 ml PBS and centrifuged at 500*g* for 10 min. The cells were stained for flow cytometry analysis.

Flow cytometry analysis

Cells (1×10^5) were suspended in 50 μl FACS buffer (0.5% BSA in PBS) for cell surface marker analysis. The cell suspensions were incubated with anti-CD16/CD32 (BioLegend; clone 93, 5 ng μl^{-1}) for 10 min at 4 °C to prevent nonspecific binding . This was followed by staining with the appropriate antibodies for 30 min at 4 °C. For extracellular staining, antibodies to the following surface markers were used: CD3 (BioLegend, clone 17A2; 2 ng μl^{-1}), CD4 (BioLegend, clone GK1.5; 2 ng μl^{-1}), CD8a (BioLegend, clone 53–7.6; 2 ng μl^{-1}), TCR-β (BioLegend, clone H57-597; 2 ng μl^{-1}), TCR-γδ (BioLegend, clone GL3; 2 ng μl^{-1}), CD45 (Invitrogen, clone 30F-11; 5 ng μl^{-1}; or BioLegend, clone 30F-11; 2 ng μl^{-1}), CD11b (BioLegend, clone M1/70; 0.6 ng μl^{-1}), CX3CR1 (BioLegend, clone SA011F11; 2 ng μl^{-1}), dectin-1 (Abcam, clone 2A11; 1 ng μl^{-1}), Ly6C (BioLegend, clone HK1.4; 2 ng μl^{-1}) and MHC-II (BioLegend, clone M5/114.15.2; 2 ng μl^{-1}). The monoclonal antibody to Vγ6 (1C10-1F7 clone; 18 ng μl^{-1}) was purified from the hybridoma supernatant using a mouse TCS purification system (Abcam) as previously reported[70]. The monoclonal antibody was conjugated to Alexa Fluor 647 using a labeling kit (Invitrogen). TCR Vγ7 (BioLegend, clone F2.67; 5 ng μl^{-1}) was used for staining and followed by reaction with Alexa Fluor 488 anti-mouse IgG2a (BioLegend, clone RMG2a-62; 2.5 ng μl^{-1}). In preparation for intracellular staining, cells were first incubated with 0.2% eBiolegend cell

stimulation cocktail (plus protein transport inhibitors; Invitrogen) in RPMI 1640 medium containing 10% fetal bovine serum at 37 °C for 6 h. The cells were then stained for the surface markers as detailed above, followed by fixation and permeabilization via their respective buffers as per the manufacturer's instructions. Briefly, the cells were fixed for 15 min at 4 °C and washed with Permeabilization Buffer (eBiosciences). The cells were then incubated for 30 min with the pertinent antibodies in Permeabilization Buffer at 4 °C. Here the antibodies to FOXP3 (Invitrogen, clone FJK-16s; 2 ng μl^{-1}), IL-1β (Invitrogen, clone NJTEN3; 5 ng μl^{-1}), IL-17a (Invitrogen, clone eBio17B7; 2 ng μl^{-1}) and IL-23 p19 (Invitrogen, clone fc23cpg; 2 ng μl^{-1}) were used. All antibodies used for flow cytometry analysis are listed in Supplementary Table 5. After incubation the cells were washed and then resuspended in 300 μl FACS buffer. The initial analysis of the cells was conducted using a MACSQuant Analyzer 10 cytometer (Miltenyi Biotec). Further analysis was performed using the FlowJo software (version 10.7, BD Biosciences). Gates were validated by 7-AAD viability staining solution, and LIVE/DEAD fixable green, red and aqua dead cell stain kits (all from Invitrogen) to identify live and dead cells. Samples were acquired and analyzed by an investigator unaware of the treatment groups.

Immunohistochemistry and image analysis

Immunohistochemical analysis of colon samples was performed using a published protocol[71]. Briefly, mice were anesthetized with isoflurane and perfused transcardially with ice-cold PBS, followed by 4% paraformaldehyde. After replacement of the paraformaldehyde with 30% sucrose in PBS, the fixed colon was embedded in cryocompound (Sakura Finetek USA). Colonic sections (20 μm) were obtained with a cryostat (cat no. CM 3050S, Leica). The sections were washed with PBS containing 0.5% Triton X-100, followed by blocking with 0.5% Triton X-100 containing 1% normal goat serum for 1 h. After blocking the sections were incubated overnight with Armenian hamster FITC-labeled anti-TCR-γδ (cat no. ab118864, Abcam; 1:100), Armenian hamster anti-TCR-γδ (cat no. 118101, BioLegend; 1:100) or rat anti-GFP (cat no. 04404-84, Nacalai; 1:1,000) at 4 °C. An additional incubation with secondary antibodies conjugated to either Alexa 488 (cat no. A-11006, Invitrogen; 1:400) or Alexa 568 (cat no. A-21112, Invitrogen; 1:400) was performed for 2 h. Nuclei were labeled with DAPI (cat no. 10236276001, Roche). For intact skull immunohistochemistry, mice were anesthetized with isoflurane and perfused transcardially with ice-cold PBS, followed by 4% paraformaldehyde. The skull was isolated via the removal of the mandibles as well as the surrounding skin and muscle. Skull decalcification was performed as previously described[15]. Consecutive coronal sections (20-μm thick) were cut using a cryostat. The sections were boiled in HistoVT One solution (cat no. 06380-05, Nacalai Tesque) for 30 min at 60 °C for antigen retrieval. The sections were then washed with PBS containing 0.5% Triton X-100, followed by blocking with 0.5% Triton X-100 containing 1% normal goat serum for 1 h. After blocking, the sections were incubated overnight with rabbit anti-laminin (cat no. L9393, Millipore Sigma; 1:100) and Armenian hamster FITC-labeled anti-TCR-γδ (cat no. ab118864, Abcam; 1:100) or rat anti-GFP (cat no. 04404-84, Nacalai; 1:1,000) at 4 °C. An additional incubation with secondary antibodies conjugated to Alexa 488 (cat no. A-11006, Invitrogen; 1:400) and Alexa 568 (cat no. A-11011, Invitrogen; 1:400) was performed for 2 h. Nuclei were labeled with DAPI. All antibodies used for immunohistochemical analysis are listed in Supplementary Table

5. Immunofluorescence images were acquired using a Zeiss LSM700 confocal microscope with the ZEN 2010 software (Carl Zeiss). Five mice were used for quantification for each group. The immunofluorescence was calculated by the FIJI package for ImageJ. Identical parameters for all imaging and threshold settings were used for all groups to minimize experimental bias.

Isolation of γδ T cells and adoptive transfer

Positive magnetic cell sorting using a γδ T cell isolation kit (Miltenyi Biotec) was used to purify γδ T cells from the splenic cells of eight-week-old mice. Sorted cells were spun down and washed with PBS for the following experiments. For adoptive transfer experiments, 1×10^6 purified γδ T cells were transferred twice by i.v. injection into mice, grouped as indicated, 1 d before and 5 d after the start of CSDS. The mice in the control group were simultaneously injected with PBS.

Anti-TCR-γδ treatment

For the antibody-mediated inhibition experiments, animals were treated monoclonal antibody (50 μg per mouse) to TCR-γδ (UC7-13D5, BioXCell) or its isotype control (BioXCell) via i.p. injection 1 d before the start of CSDS.

Statistics

Statistical differences among three independent groups were determined using a one-way ANOVA, followed by Tukey's multiple-comparison test. An unpaired two-tailed Student's *t*-test was used to compare two sets of data. For comparisons of multiple factors, a two-way ANOVA with Tukey's multiple comparisons tests was used. Sample sizes were chosen on the basis of a power analysis using estimates from previously published experiments[6,22]. Randomization was not relevant to the clinical findings as this was an observational cohort. The animals were randomly assigned to groups before the start of experimentation and investigators were blinded to allocation during experiments and outcome assessment. No data were excluded. All data from animal experiments are presented as the mean ± s.e.m. Spearman's correlation analysis was used to evaluate the relationships between two continuous variables. Multivariable regression analysis was performed to evaluate the association between the relative abundance of *Lactobacillus* in patients with MDD and multiple variables that include antidepressant dosage, sex, age, body mass index and the duration since the first episode of depression. Statistical analyses were conducted using GraphPad Prism 9 (GraphPad Software) and IBM SPSS Statistics version 25.0 (SPSS Inc.), as appropriate. For the human study, continuous and categorical variables were described as the mean ± s.d. and percentages, respectively. All variables were inspected to test the data distribution using histograms, Q–Q plots and Kolmogorov–Smirnov tests before conducting statistical analyses. Independent *t*-tests were used to compare differences in demographics and clinical characteristics at baseline. A categorical variable was compared using Pearson's χ^2 test. A value of $P < 0.05$ was considered to be significant. All detailed additional statistic information is shown in Supplementary Table 4.

Extended Data

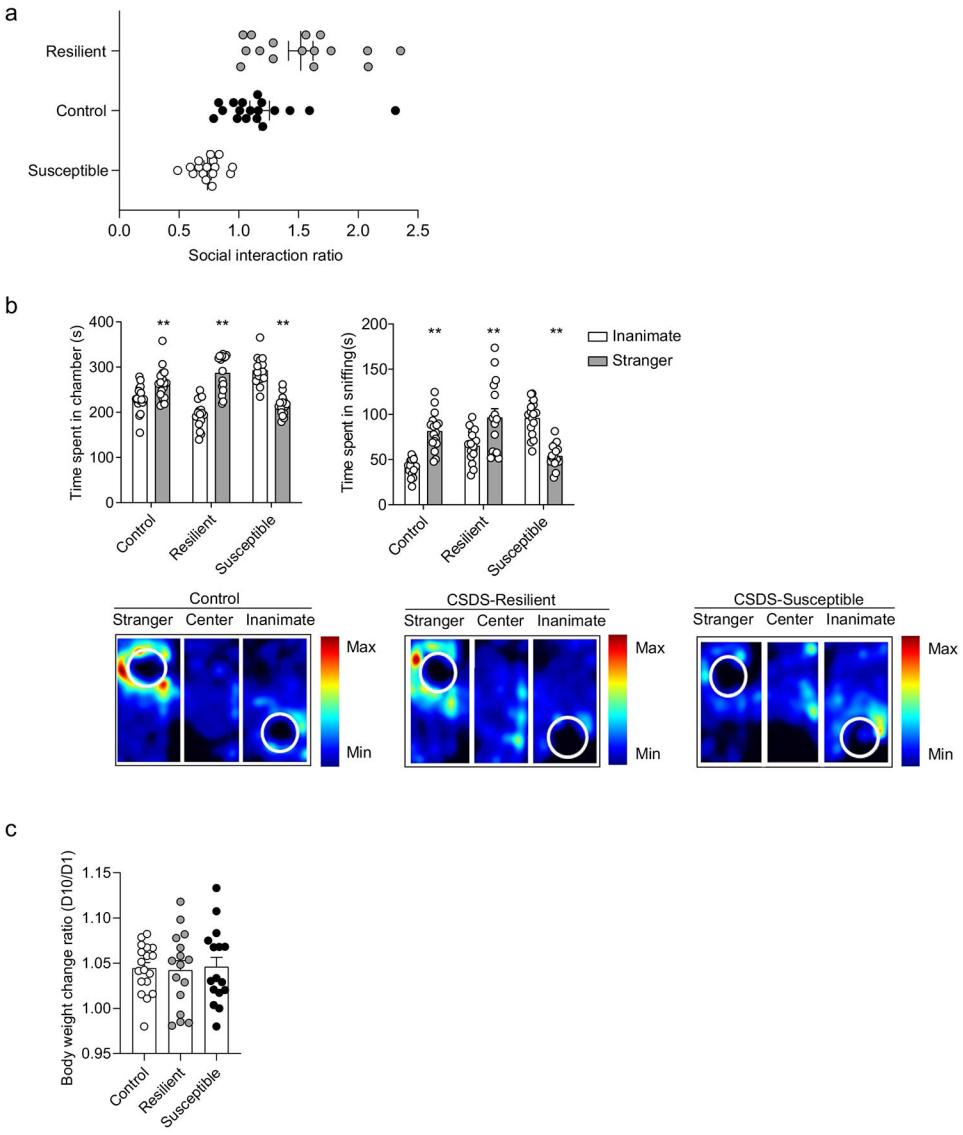

Extended Data Fig. 1 |. CSDS-induced social-avoidance phenotype assessed using a three-chamber social interaction test.

a, CSDS results in a spectrum of social-avoidance behavior, divided between susceptible and resilient phenotypes using their social interaction ratio (SIR) score. **b**, Time the mice spent in the chamber with an inanimate object versus with a stranger mouse (top left). Time the mice spent sniffing an inanimate object versus a stranger mouse (top right). Representative heatmaps depict movements of the control, resilient and susceptible mice (bottom). **c**, Body-weight change ratio of control, resilient and susceptible mice between before and after CSDS. **a**–**c**, $n = 18$ control mice, $n = 16$ resilient mice and $n = 16$ susceptible mice. $^{**}P < 0.01$ (time spent in chambers: $P = 0.0067$, $P < 0.0001$, $P < 0.0001$; time spent sniffing: $P < 0.0001$, $P = 0.0006$ and $P < 0.0001$), determined using an unpaired two-tailed Student's *t*-test. Error bars represent the mean ± s.e.m.

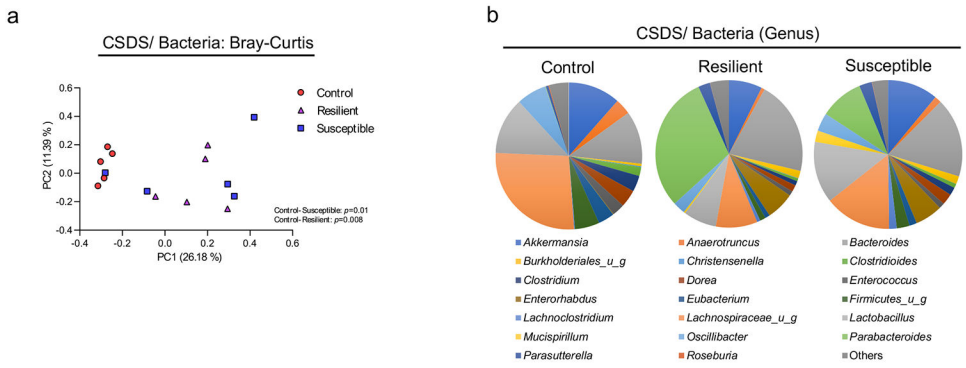

Extended Data Fig. 2 |. CSDS induces alteration of intestinal bacteria.

a, Bray–Curtis β-diversity index of grouped data of fecal bacteria at the species level (n = 5 per group). Analyzed by one-way ANOVA with Tukey's post-hoc test; adjustments were made for multiple comparisons. **b**, Relative abundance of fecal bacteria at the genus level in control, resilient and susceptible mice (n = 5 per group). For details about altered species across conditions, refer to Supplementary Table 1.

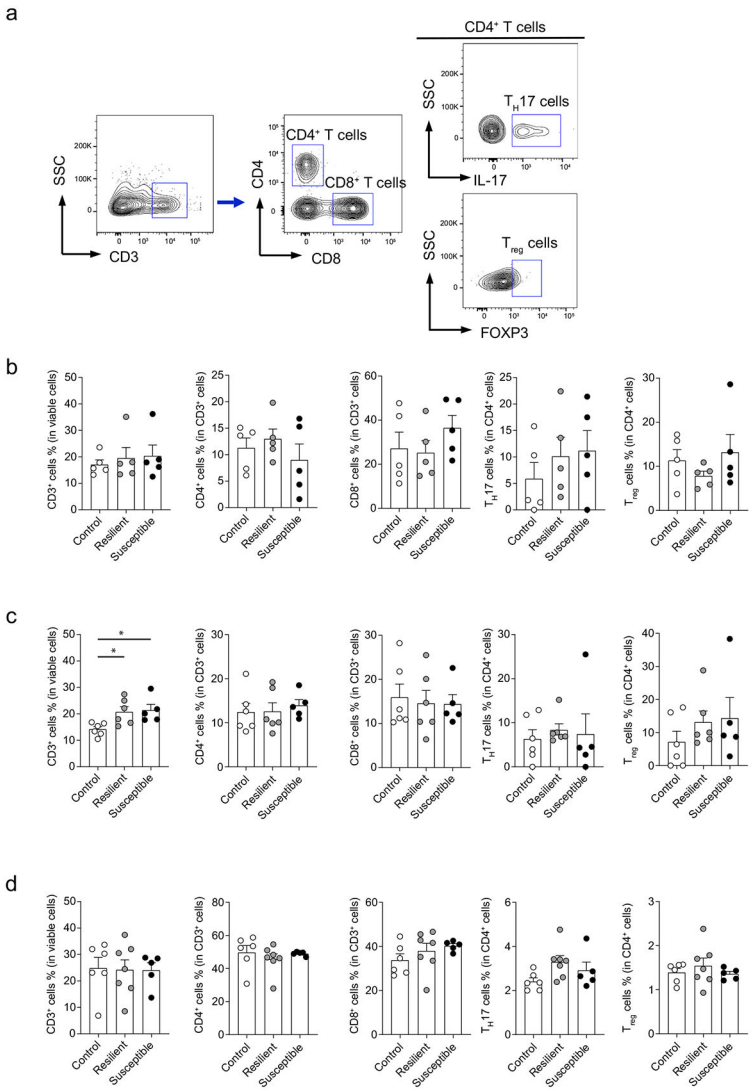

Extended Data Fig. 3 |. The effect of CSDS on other T cell subtypes in the colon, small intestine and spleen.

a, Representative flow cytometry plots of $CD3^+$ T cells, $CD4^+$ T cells ($CD3^+CD4^+$), $CD8^+$ T cells ($CD3^+CD8^+$), T_H17 cells ($CD3^+CD4^+IL\text{-}17^+$) and T_{reg} cells ($CD3^+CD4^+FOXP3^+$) in the LP of the colon. **b**–**d**, Percentages of $CD3^+$ T cells in viable cells, $CD4^+$ T cells in $CD3^+$ T cells, $CD8^+$ T cells in $CD3^+$ T cells, T_H17 cells in $CD4^+$ T cells and T_{reg} cells in $CD4^+$ T cells in the LP of the colon (**b**; $n = 5$, 5 and 5), small intestine (**c**; $n = 6$, 6 and 5) and spleen (**d**; $n = 6$, 7 and 5) of control, resilient and susceptible mice. $^*P < 0.05$ (P values are $P = 0.031$ and $P = 0.0402$), determined by one-way ANOVA with Tukey's post-hoc test. Error bars represent the mean ± s.e.m.

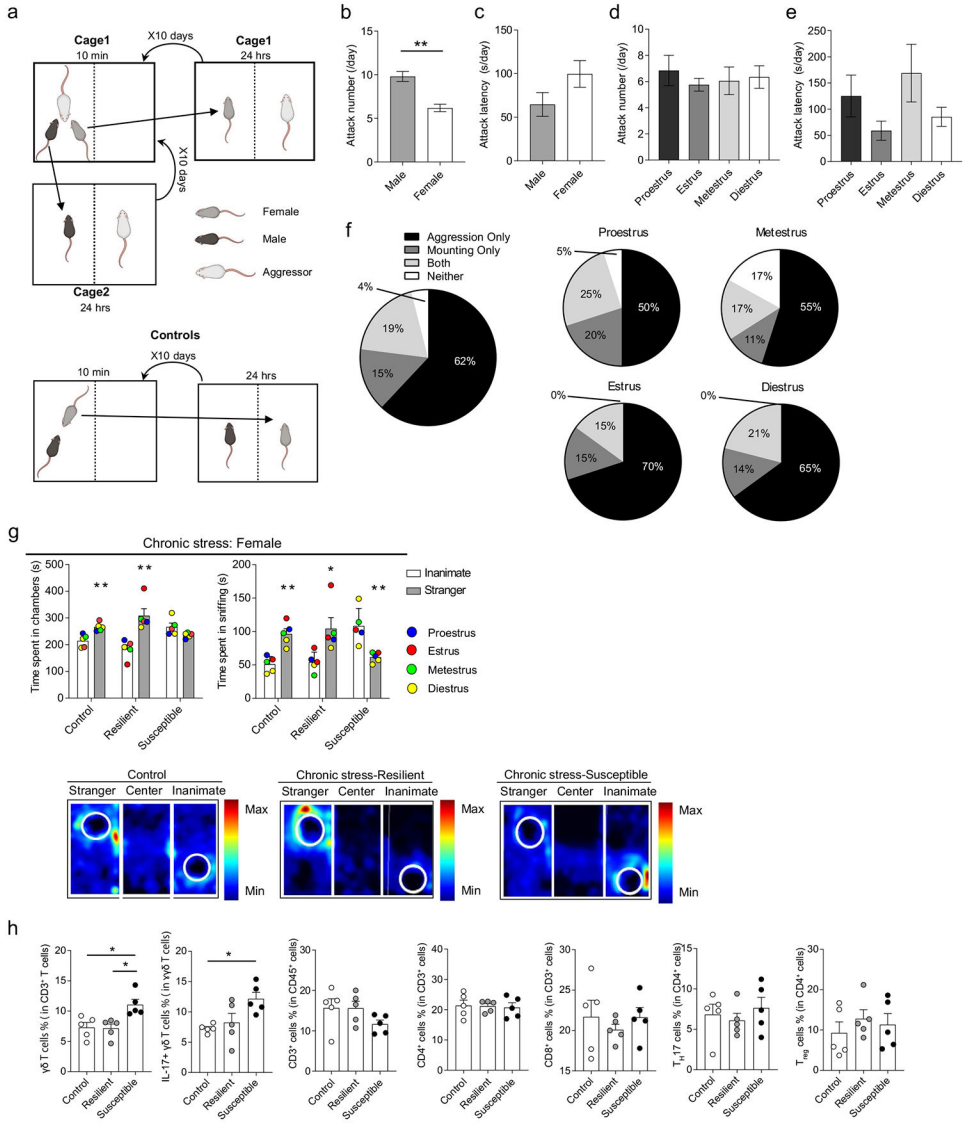

Extended Data Fig. 4 |. CSDS-induced changes in T cells and social avoidance in female mice. **a**, Schematic representation of chronic stress paradigm for female mice. **b**,**c**, Attack number (**b**) and latency (**c**) of CD-1 aggressors on male versus female mice. $n = 100$ (ten mice × 10 d) per group. **d**,**e**, Attack number (**d**) and latency (**e**) of CD-1 aggressors during the proestrus ($n = 20$), estrus ($n = 33$), metestrus ($n = 18$) and diestrus ($n = 29$) cycle of female mice. **f**, The percentage of CD-1 behaviors directed towards female mice over the 10-d chronic stress period (left) and over the course of the estrous cycle (middle and right). **g**, Time the mice spent in the chamber with an inanimate object versus a stranger female mouse (top left). Time the mice spent sniffing an inanimate object versus a stranger female mouse (top right). The color in the dots represents the estrous cycle of the test female mouse. Representative heatmaps depict mice movements (bottom). Control, resilient and susceptible mice ($n = 5$, 5, 5). **h**, Percentage of γδ T cells in $CD3^+$ T cells, γδ17 T cells in γδ T cells, $CD3^+$ T cells in viable cells, $CD4^+$ T cells in $CD3^+$ T cells, $CD8^+$ T cells in $CD3^+$ T cells, T_H17 cells in $CD4^+$ T cells and T_{reg} cells in $CD4^+$ T cells in the meninges of control, resilient

and susceptible female mice (n = 5, 5, 5). **b**,**g**, *P < 0.05 and **P < 0.01 (**b**, P < 0.0001; **g**, time spent in chambers: P = 0.0039 and P = 0.0033; time spent sniffing: P = 0.0012, P = 0.0237 and P = 0.0049), determined using an unpaired two-tailed Student's t-test. **h**, *P < 0.05 (percentage γδ T cells: P = 0.0158, P = 0.0126; percentage γδ17 T cells: P = 0.0203), determined by one-way ANOVA with Tukey's post-hoc test. Error bars represent the mean ± s.e.m.

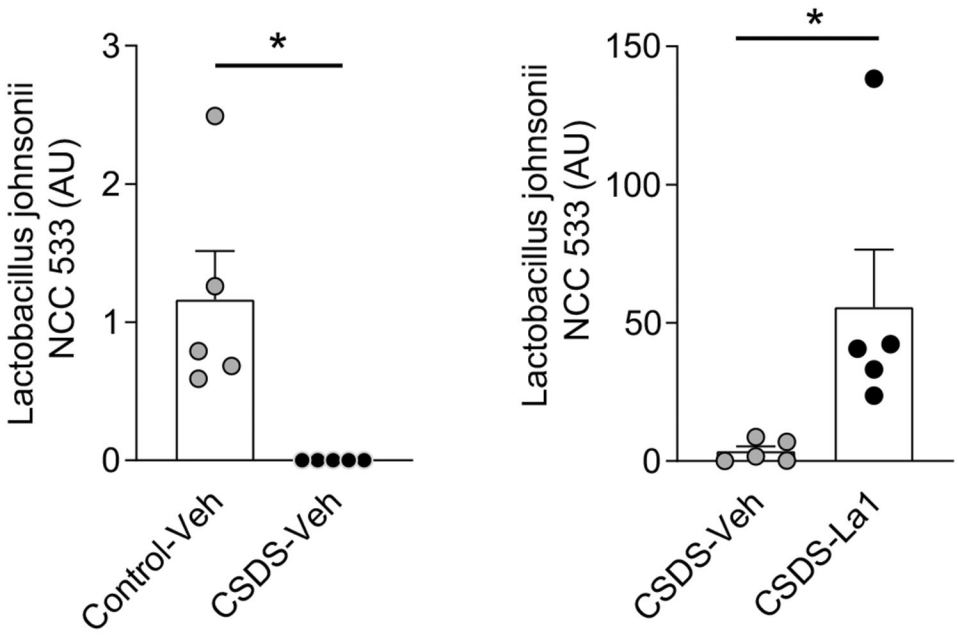

Extended Data Fig. 5 |. Quantification of La1 in the colonic fecal samples by quantitative real time PCR.

The graphs represent the La1 level in the fecal samples collected from the colon of ctr + vehicle and CSDS + vehicle groups of mice (n = 5, 5; left) as well as the colon of CSDS + vehicle and CSDS + La1 groups of mice (n = 5, 5; right). *P < 0.05 (P = 0.0039 and P = 0.0142), determined by an unpaired two-tailed Student's t-test. Error bars represent the mean ± s.e.m.

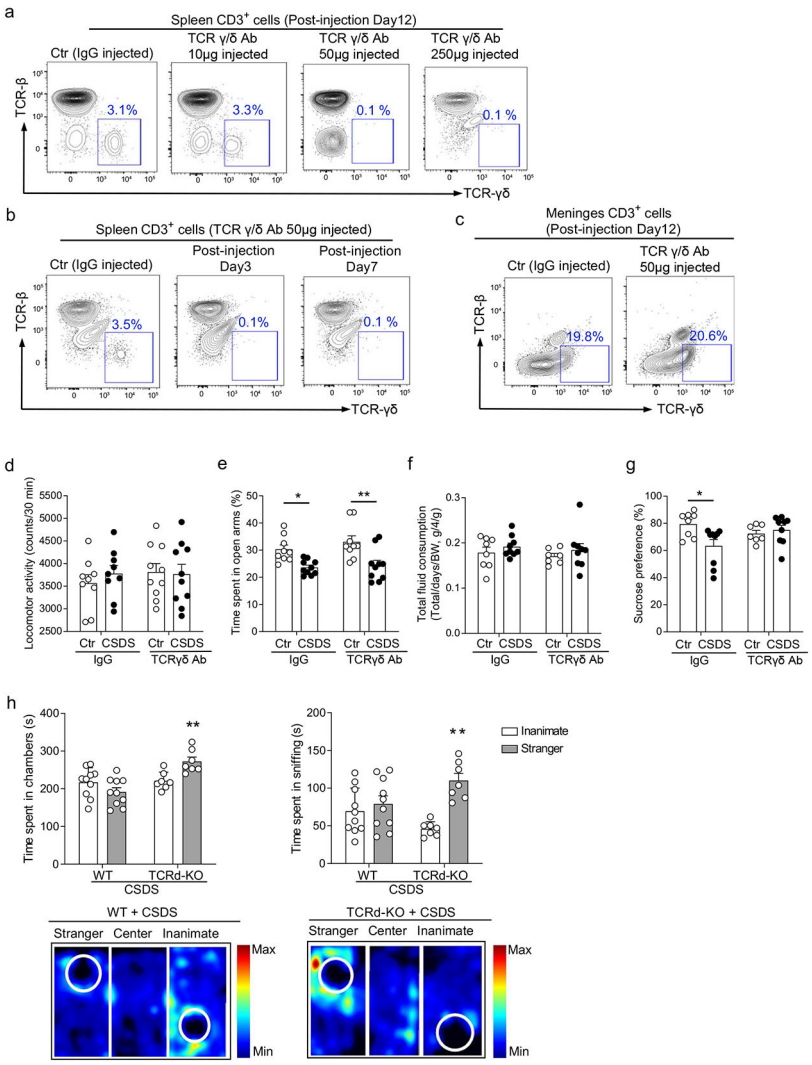

Extended Data Fig. 6 |. Inhibition effects of i.p. injection of anti-TCR-γδ on γδ T cells in the spleen and meninges as well as CSDS-induced behaviors and the effect of genetic deletion of TCRd on CSDS-induced social-avoidance behavior.

a, Representative flow cytometry plots of γδ T cells ($CD3^+TCR\text{-}\beta^-TCR\text{-}\gamma\delta^+$) in the spleen of WT mice injected with IgG or anti-TCR-γδ (10, 50 and 250 μg per mouse, respectively) at post-injection day 12. **b**, Representative flow cytometry plots of γδ T cells in the spleen of WT mice injected with IgG or anti-TCR-γδ (50 μg per mouse) at post-injection days 3 and day 7, respectively. **c**, Representative flow cytometry plots of γδ T cells in the meninges of WT mice injected with IgG or anti-TCR-γδ (50 μg per mouse) at post-injection day 12. The boxes in the dot plots identify γδ T cells and represent the percentage of γδ T cells in $CD3^+$ T cells in all groups of mice. **d**, Locomotion activity as assessed by total counts in the OFT of ctr + IgG, CSDS + IgG, ctr + anti-TCR-γδ and CSDS + anti-TCR-γδ groups of mice (n = 9, 9, 10 and 10). **e**, Percentage of time spent in the open arms during the elevated plus maze (EPM) test of mice: ctr + IgG, CSDS + IgG, ctr + anti-TCR-γδ and CSDS + anti-TCR-γδ (n = 9, 10, 9 and 10). **f**,**g**, The average of total fluid consumption **(f)** and the average percentage of sucrose consumption when given a choice between 1.5%

sucrose and water (**g**) on days 5–8 of ctr + IgG, CSDS + IgG, ctr + anti-TCR-γδ and CSDS + anti-TCR-γδ groups of mice (n = 8, 9, 7, 9). **h**, Time test mice spend in the chambers (top left). Time test mice spent sniffing (top right). Representative heatmaps depicting mice movements (bottom). n = 10 for WT + CSDS and n = 7 for TCRd-KO + CSDS groups of mice. **e**,**g**, $*P < 0.05$ and $**P < 0.01$ (**e**, $P = 0.0384$ and $P = 0.0045$; **g**, $P = 0.0207$), determined by two-way ANOVA with Tukey's post-hoc test. **h**, $**P < 0.01$ (time spent in chambers: $P = 0.0041$; time spent in sniffing: $P < 0.0001$), determined by an unpaired two-tailed Student's t-test. Error bars represent the mean ± s.e.m.

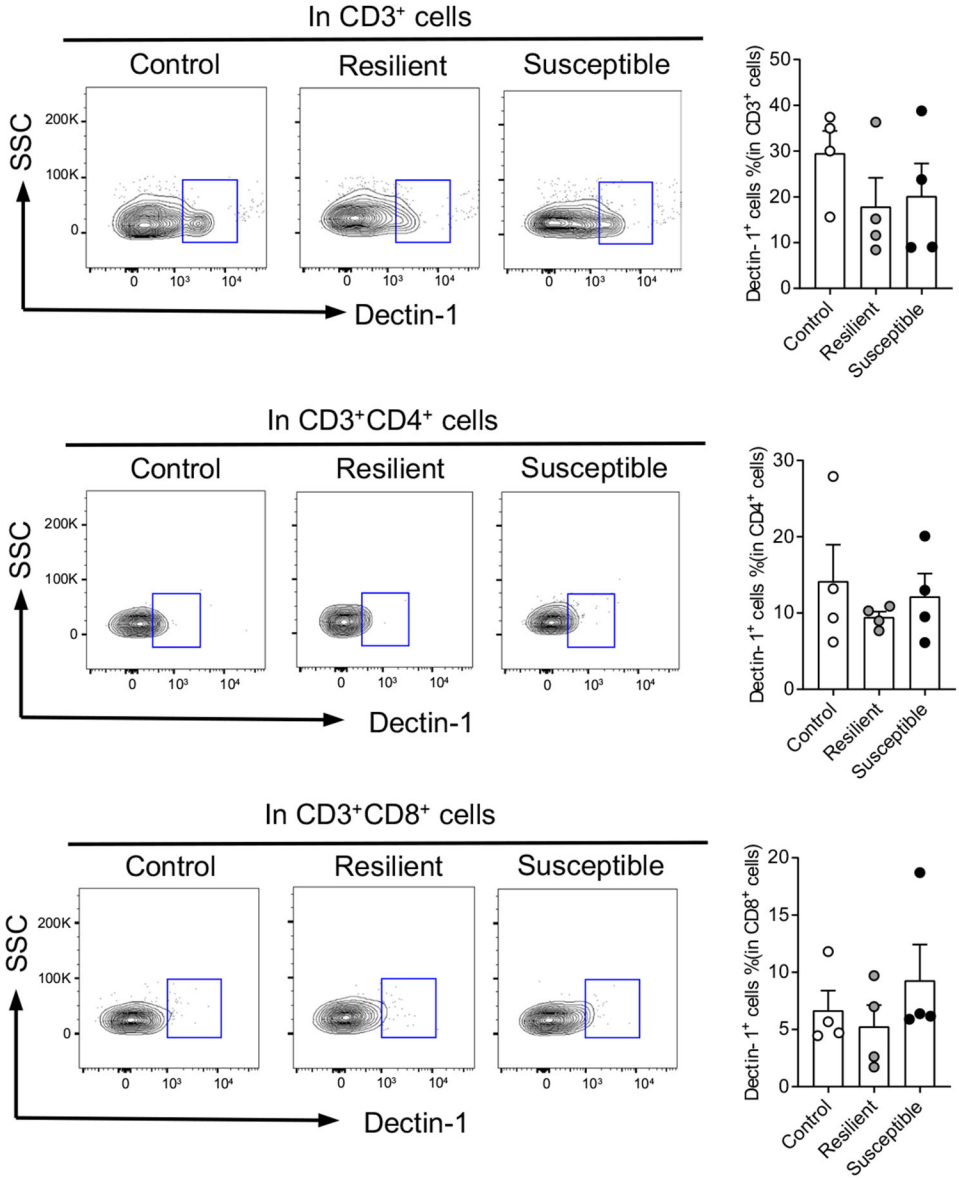

Extended Data Fig. 7 |. No change in dectin-1 expression in the colonic CD3$^+$, CD4$^+$ and CD8$^+$ T cells of C57BL/6 mice after CSDS.

Representative flow cytometry plots (left). Percentage of dectin-1$^+$ cells in CD3$^+$ (top right), CD4$^+$ (middle right) and CD8$^+$ (bottom right) T cells in the LP of the colon of control,

resilient and susceptible mice (n = 4, 4, 4). The boxes in the dot plots identify dectin-1$^+$ cells in each group of mice. Error bars represent the mean ± s.e.m.

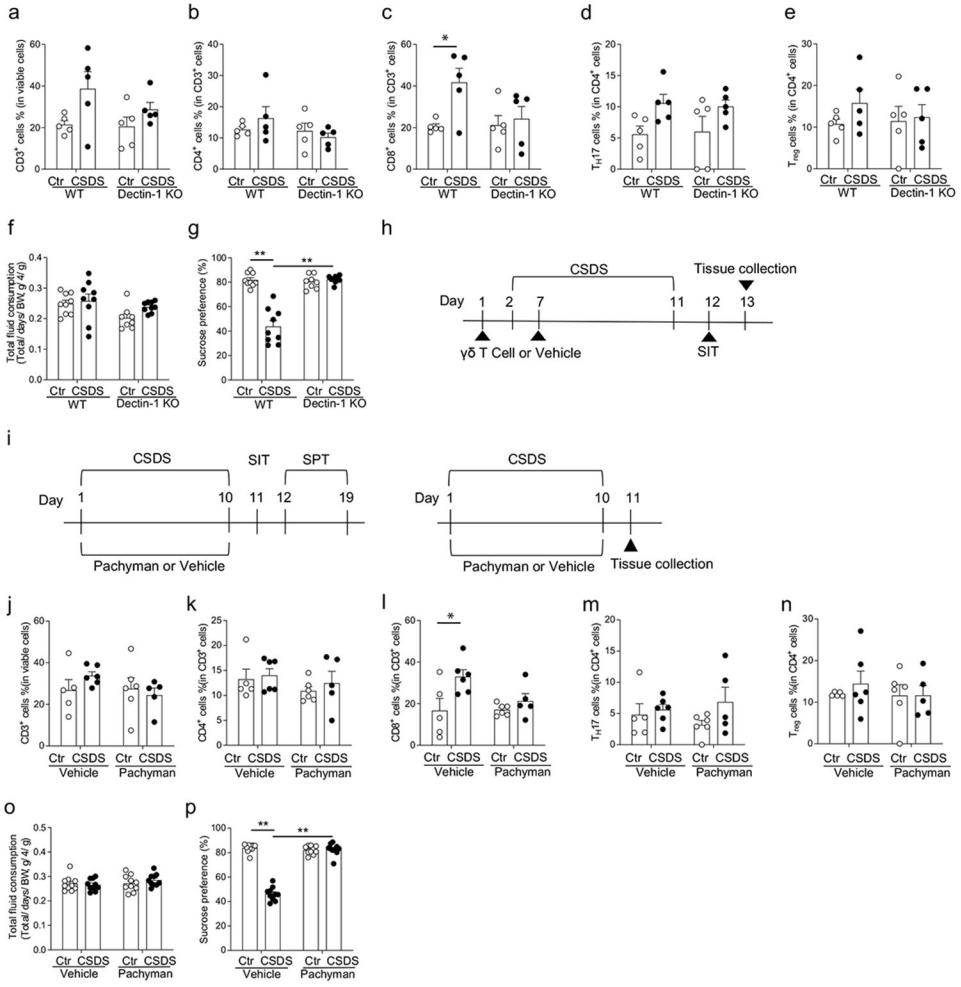

Extended Data Fig. 8 |. The effects of genetic deletion of dectin-1 and treatment with pachyman on CSDS-induced phenotypes in colonic non-γδ T lymphocytes and sucrose preference test. **a**–**e**, Percentage of CD3$^+$ T cells in viable cells (**a**), CD4$^+$T cells in CD3$^+$ cells (**b**), CD8$^+$ T cells in CD3$^+$ cells (**c**), T_H17 cells in CD4$^+$ cells (**d**) and T_{reg} cells in CD4$^+$ cells (**e**) in the LP of the colon of WT + ctr, WT + CSDS, dectin-1 KO + ctr and dectin-1 KO + CSDS groups of mice (n = 5, 5, 5, 5). **f**,**g**, The average of total fluid consumption (**f**) and the average percentage of sucrose consumption when given a choice between 1.5% sucrose and water (**g**) on days 5–8 for WT + ctr, WT + CSDS, dectin-1 KO + ctr and dectin-1 KO + CSDS groups of mice (n = 9, 9, 8, 9). **h**, Schematic of the experimental design. Eight-week-old TCRd-KO mice received i.v. injection of γδ T cells collected from *Clec7a*$^{-/-}$ (dectin-1 KO) mice or their WT littermates 1 d before and 5 d after the start of CSDS, followed by a social interaction test (SIT) and tissue collection. **i**, Schematic of the experimental design. Eight-week-old C57BL/6 mice were orally treated with the vehicle or pachyman daily during the CSDS period, followed by SIT and sucrose preference test (SPT; left). An independent cohort of mice was subjected to tissue harvest 1 d after CSDS (right).

j–**n**. Percentage of $CD3^+$ cells in viable cells (**j**), $CD4^+$ cells in $CD3^+$ cells (**k**), $CD8^+$ cells in $CD3^+$ cells (**l**), T_H17 cells in $CD4^+$ cells (**m**) and T_{reg} cells in $CD4^+$ cells (**n**) in the LP of the colon of ctr + vehicle, CSDS + vehicle, ctr + pachyman and CSDS + pachyman groups of mice ($n = 5, 6, 6, 5$). **o**,**p**, The average of total fluid consumption (**o**) and the average percentage of sucrose consumption when given a choice between 1.5% sucrose and water (**p**) on days 5–8 for four groups of mice: ctr + vehicle, CSDS + vehicle, ctr + pachyman and CSDS + pachyman ($n = 10, 10, 10$ and 10). *$P < 0.05$ and **$P < 0.01$ (**c**, $P = 0.0429$; **g**, $P < 0.0001$ and $P < 0.0001$; **l**, $P = 0.0252$; **p**, $P < 0.0001$ and $P < 0.0001$), determined by two-way ANOVA with Tukey's post-hoc test. Error bars represent the mean ± s.e.m.

Supplementary Material

Refer to Web version on PubMed Central for supplementary material.

Acknowledgements

We thank S. Poynton and S. Madireddy for critical reading of the manuscript. We thank Y. Iwakura (Tokyo University of Science), R. Giger (University of Michigan) and T. Hohl (Sloan Kettering Institute) for providing us with *Clec7a*$^{-/-}$ mice. We thank the Johns Hopkins University School of Medicine (JHU SOM) Flow Cytometry Core Facility, the JHU SOM Microscopy Core Facility and the JHU SOM Behavioral Core Facility. We thank S. Duboux (Société des Produits Nestlé S.A.) and Y. Fukushima (Nestlé Japan Manufacturing, Tokyo, Japan) for their help with culturing *L. johnsonii* La1, which was supplied from NESTEC. LTD (Lausanne, Switzerland). Some elements in Fig. 4a and Extended Data Fig. 4a were created using BioRender.com (2021). We also thank D. Tamura for providing a gift fund. This work was supported by grants from the National Institute of Health Awards grant nos DA041208 (A.K.), AG065168 (A.K.), MH094268 (A.K.), MH128765 (A.K.), AT008547 (A.K.), AT010984 (X.Z.), NS041435 (P.A.C.) and MH113645 (S.-i.K.) as well as institutional and foundation grants from the JHU catalyst award (A.K.), JSCNP (S.S.), Kanae (Y.H.), JST ERATO (grant no. JPMJER1902; S.F.), AMED-CREST (grant no. JP22gm1010009; S.F.), JSPS KAKENHI (grant no. 22H03541; S.F.), the Food Science Institute Foundation (S.F.) and the Japan Dairy Association (J-milk) (K.S.).

Data availability

The raw data of the shotgun metagenomic sequencing of mouse fecal samples that support the findings of this study have been deposited to NCBI Sequence Read Archive under BioProject PRJNA758357. The *16S* rRNA gene sequences obtained from human fecal samples have been deposited to the DNA DataBank of Japan (DDBJ) under the accession number DRA010810 (patients with MDD) and DRA012712 (healthy controls). Human data have been de-identified to protect confidentiality. The SILVA132 database can be downloaded at https://www.arb-silva.de/fileadmin/silva_databases/qiime/Silva_132_release.zip. Source data are provided with this paper.

References

1. Hodes GE et al. Individual differences in the peripheral immune system promote resilience versus susceptibility to social stress. Proc. Natl Acad. Sci. USA 111, 16136–16141 (2014). [PubMed: 25331895]
2. McKim DB et al. Microglial recruitment of IL-1β-producing monocytes to brain endothelium causes stress-induced anxiety. Mol. Psychiatry 23, 1421–1431 (2018). [PubMed: 28373688]
3. Nie X et al. The innate immune receptors TLR2/4 mediate repeated social defeat stress-induced social avoidance through prefrontal microglial activation. Neuron 99, 464–479 (2018). [PubMed: 30033154]

4. Pearson-Leary J et al. The gut microbiome regulates the increases in depressive-type behaviors and in inflammatory processes in the ventral hippocampus of stress vulnerable rats. Mol. Psychiatry 25, 1068–1079 (2020). [PubMed: 30833676]
5. Haroon E, Raison CL & Miller AH Psychoneuroimmunology meets neuropsychopharmacology: translational implications of the impact of inflammation on behavior. Neuropsychopharmacology 37, 137–162 (2012). [PubMed: 21918508]
6. Sakamoto S et al. Alterations in circulating extracellular vesicles underlie social stress-induced behaviors in mice. FEBS Open Bio 11, 2678–2692 (2021).
7. Biltz RG, Sawicki CM, Sheridan JF & Godbout JP The neuroimmunology of social-stress-induced sensitization. Nat. Immunol 23, 1527–1535 (2022). [PubMed: 36369271]
8. Ribot JC, Lopes N & Silva-Santos B γδ T cells in tissue physiology and surveillance. Nat. Rev. Immunol 21, 221–232 (2021). [PubMed: 33057185]
9. Jin C et al. Commensal microbiota promote lung cancer development via γδ T cells. Cell 176, 998–1013 (2019). [PubMed: 30712876]
10. Shichita T et al. Pivotal role of cerebral interleukin-17-producing γδT cells in the delayed phase of ischemic brain injury. Nat. Med 15, 946–950 (2009). [PubMed: 19648929]
11. Dupraz L et al. Gut microbiota-derived short-chain fatty acids regulate IL-17 production by mouse and human intestinal γδ T cells. Cell Rep. 36, 109332 (2021). [PubMed: 34233192]
12. Filiano AJ et al. Unexpected role of interferon-γ in regulating neuronal connectivity and social behaviour. Nature 535, 425–429 (2016). [PubMed: 27409813]
13. Alves de Lima K et al. Meningeal γδ T cells regulate anxiety-like behavior via IL-17a signaling in neurons. Nat. Immunol 21, 1421–1429 (2020). [PubMed: 32929273]
14. Ribeiro M et al. Meningeal γδ T cell-derived IL-17 controls synaptic plasticity and short-term memory. Sci. Immunol 4, eaay5199 (2019). [PubMed: 31604844]
15. Benakis C et al. Commensal microbiota affects ischemic stroke outcome by regulating intestinal γδ T cells. Nat. Med 22, 516–523 (2016). [PubMed: 27019327]
16. Choi GB et al. The maternal interleukin-17a pathway in mice promotes autism-like phenotypes in offspring. Science 351, 933–939 (2016). [PubMed: 26822608]
17. Medina-Rodriguez EM et al. Identification of a signaling mechanism by which the microbiome regulates Th17 cell-mediated depressive-like behaviors in mice. Am. J. Psychiatry 177, 974–990 (2020). [PubMed: 32731813]
18. Brown GD Dectin-1: a signalling non-TLR pattern-recognition receptor. Nat. Rev. Immunol 6, 33–43 (2006). [PubMed: 16341139]
19. Martin B, Hirota K, Cua DJ, Stockinger B & Veldhoen M Interleukin-17-producing γδ T cells selectively expand in response to pathogen products and environmental signals. Immunity 31, 321–330 (2009). [PubMed: 19682928]
20. Kamiya T et al. β-Glucans in food modify colonic microflora by inducing antimicrobial protein, calprotectin, in a Dectin-1-induced-IL-17F-dependent manner. Mucosal Immunol. 11, 763–773 (2018). [PubMed: 29068000]
21. Tang C et al. Inhibition of Dectin-1 signaling ameliorates colitis by inducing *Lactobacillus*-mediated regulatory T cell expansion in the intestine. Cell Host Microbe 18, 183–197 (2015). [PubMed: 26269954]
22. Zhu X et al. JHU-083 selectively blocks glutaminase activity in brain $CD11b^{+}$ cells and prevents depression-associated behaviors induced by chronic social defeat stress. Neuropsychopharmacology 44, 683–694 (2019). [PubMed: 30127344]
23. Burokas A et al. Targeting the microbiota–gut–brain axis: prebiotics have anxiolytic and antidepressant-like effects and reverse the impact of chronic stress in mice. Biol. Psychiatry 82, 472–487 (2017). [PubMed: 28242013]
24. Gao X et al. Chronic stress promotes colitis by disturbing the gut microbiota and triggering immune system response. Proc. Natl Acad. Sci. USA 115, E2960–E2969 (2018). [PubMed: 29531080]
25. Lee YK, Menezes JS, Umesaki Y & Mazmanian SK Proinflammatory T-cell responses to gut microbiota promote experimental autoimmune encephalomyelitis. Proc. Natl Acad. Sci USA 108, 4615–4622 (2011). [PubMed: 20660719]

26. Atarashi K et al. Induction of colonic regulatory T cells by indigenous *Clostridium* species. Science 331, 337–341 (2011). [PubMed: 21205640]
27. Yohn CN et al. Chronic non-discriminatory social defeat is an effective chronic stress paradigm for both male and female mice. Neuropsychopharmacology 44, 2220–2229 (2019). [PubMed: 31493767]
28. Harris AZ et al. A novel method for chronic social defeat stress in female mice. Neuropsychopharmacology 43, 1276–1283 (2018). [PubMed: 29090682]
29. Nielsen MM, Witherden DA & Havran WL γδ T cells in homeostasis and host defence of epithelial barrier tissues. Nat. Rev. Immunol 17, 733–745 (2017). [PubMed: 28920588]
30. Vantourout P & Hayday A Six-of-the-best: unique contributions of γδ T cells to immunology. Nat. Rev. Immunol 13, 88–100 (2013). [PubMed: 23348415]
31. Taylor PR et al. Dectin-1 is required for β-glucan recognition and control of fungal infection. Nat. Immunol 8, 31–38 (2007). [PubMed: 17159984]
32. Iliev ID et al. Interactions between commensal fungi and the C-type lectin receptor Dectin-1 influence colitis. Science 336, 1314–1317 (2012). [PubMed: 22674328]
33. Goodridge HS et al. Activation of the innate immune receptor Dectin-1 upon formation of a 'phagocytic synapse'. Nature 472, 471–475 (2011). [PubMed: 21525931]
34. Charlet R, Bortolus C, Sendid B & Jawhara S *Bacteroides thetaiotaomicron* and *Lactobacillus johnsonii* modulate intestinal inflammation and eliminate fungi via enzymatic hydrolysis of the fungal cell wall. Sci. Rep 10, 11510 (2020). [PubMed: 32661259]
35. Yuan N et al. An integrated pharmacology-based analysis for antidepressant mechanism of Chinese herbal formula Xiao-Yao-San. Front. Pharm 11, 284 (2020).
36. Sutton CE et al. Interleukin-1 and IL-23 induce innate IL-17 production from γδ T cells, amplifying Th17 responses and autoimmunity. Immunity 31, 331–341 (2009). [PubMed: 19682929]
37. Guo Y et al. Antidepressant effects of rosemary extracts associate with anti-inflammatory effect and rebalance of gut microbiota. Front. Pharm 9, 1126 (2018).
38. Tung TH et al. Fish oil, but not olive oil, ameliorates depressive-like behavior and gut microbiota dysbiosis in rats under chronic mild stress. Biomolecules 9, 516 (2019). [PubMed: 31546592]
39. Xie R et al. Oral treatment with *Lactobacillus reuteri* attenuates depressive-like behaviors and serotonin metabolism alterations induced by chronic social defeat stress. J. Psychiatr. Res 122, 70–78 (2020). [PubMed: 31927268]
40. Furusawa Y et al. Commensal microbe-derived butyrate induces the differentiation of colonic regulatory T cells. Nature 504, 446–450 (2013). [PubMed: 24226770]
41. Park SG et al. T regulatory cells maintain intestinal homeostasis by suppressing γδ T cells. Immunity 33, 791–803 (2010). [PubMed: 21074460]
42. Golden SA, Covington HE III, Berton O & Russo SJ A standardized protocol for repeated social defeat stress in mice. Nat. Protoc 6, 1183–1191 (2011). [PubMed: 21799487]
43. Klein SL & Flanagan KL Sex differences in immune responses. Nat. Rev. Immunol 16, 626–638 (2016). [PubMed: 27546235]
44. Salk RH, Hyde JS & Abramson LY Gender differences in depression in representative national samples: meta-analyses of diagnoses and symptoms. Psychol. Bull 143, 783–822 (2017). [PubMed: 28447828]
45. Brachman RA, Lehmann ML, Maric D & Herkenham M Lymphocytes from chronically stressed mice confer antidepressant-like effects to naive mice. J. Neurosci 35, 1530–1538 (2015). [PubMed: 25632130]
46. Fan KQ et al. Stress-induced metabolic disorder in peripheral $CD4^+$ T cells leads to anxiety-like behavior. Cell 179, 864–879 (2019). [PubMed: 31675497]
47. Papotto PH, Ribot JC & Silva-Santos B $IL\text{-}17^+$ γδ T cells as kick-starters of inflammation. Nat. Immunol 18, 604–611 (2017). [PubMed: 28518154]
48. Daley D et al. Dectin 1 activation on macrophages by galectin 9 promotes pancreatic carcinoma and peritumoral immune tolerance. Nat. Med 23, 556–567 (2017). [PubMed: 28394331]

49. Mikocka-Walus A, Ford AC & Drossman DA Antidepressants in inflammatory bowel disease. Nat. Rev. Gastroenterol. Hepatol 17, 184–192 (2020). [PubMed: 32071420]
50. Lewis K et al. The prevalence and risk factors of undiagnosed depression and anxiety disorders among patients with inflammatory bowel disease. Inflamm. Bowel Dis 25, 1674–1680 (2019). [PubMed: 30888037]
51. Hamilton M A rating scale for depression. J. Neurol. Neurosurg. Psychiatry 23, 56–62 (1960). [PubMed: 14399272]
52. Montgomery SA & Asberg M A new depression scale designed to be sensitive to change. Br. J. Psychiatry 134, 382–389 (1979). [PubMed: 444788]
53. Hamilton M The assessment of anxiety states by rating. Br. J. Med. Psychol 32, 50–55 (1959). [PubMed: 13638508]
54. Buysse DJ, Reynolds CF III, Monk TH, Berman SR & Kupfer DJ The Pittsburgh Sleep Quality Index: a new instrument for psychiatric practice and research. Psychiatry Res. 28, 193–213 (1989). [PubMed: 2748771]
55. Ishii C et al. A metabologenomic approach reveals changes in the intestinal environment of mice fed on american diet. Int. J. Mol. Sci 19, 4079 (2018). [PubMed: 30562947]
56. Kim SW et al. Robustness of gut microbiota of healthy adults in response to probiotic intervention revealed by high-throughput pyrosequencing. DNA Res. 20, 241–253 (2013). [PubMed: 23571675]
57. Bolyen E et al. Reproducible, interactive, scalable and extensible microbiome data science using QIIME 2. Nat. Biotechnol 37, 852–857 (2019). [PubMed: 31341288]
58. Quast C et al. The SILVA ribosomal RNA gene database project: improved data processing and web-based tools. Nucleic Acids Res. 41, D590–596 (2013). [PubMed: 23193283]
59. Yilmaz P et al. The SILVA and 'All-species Living Tree Project (LTP)' taxonomic frameworks. Nucleic Acids Res. 42, D643–D648 (2014). [PubMed: 24293649]
60. Denou E et al. Gene expression of commensal *Lactobacillus johnsonii* strain NCC533 during in vitro growth and in the murine gut. J. Bacteriol 189, 8109–8119 (2007). [PubMed: 17827285]
61. Mindus C, Ellis J, van Staaveren N & Harlander-Matauschek A *Lactobacillus*-based probiotics reduce the adverse effects of stress in rodents: a meta-analysis. Front. Behav. Neurosci 15, 642757 (2021). [PubMed: 34220459]
62. Inoue R, Otsuka M, Nishio A & Ushida K Primary administration of *Lactobacillus johnsonii* NCC533 in weaning period suppresses the elevation of proinflammatory cytokines and *CD86* gene expressions in skin lesions in NC/Nga mice. FEMS Immunol. Med. Microbiol 50, 67–76 (2007). [PubMed: 17425659]
63. Chu MP et al. Pachyman treatment improves $CD4^+CD25^+$ T_{reg} counts and serum interleukin 4 and interferon γ levels in a mouse model of Kawasaki disease. Mol. Med. Rep 5, 1237–1240 (2012). [PubMed: 22367425]
64. Niwa M et al. Knockdown of DISC1 by in utero gene transfer disturbs postnatal dopaminergic maturation in the frontal cortex and leads to adult behavioral deficits. Neuron 65, 480–489 (2010). [PubMed: 20188653]
65. Hasegawa Y et al. Causal impact of local inflammation in the nasal cavity on higher brain function and cognition. Neurosci. Res 172, 110–115 (2021). [PubMed: 33932551]
66. Ottesen A et al. Enrichment dynamics of *Listeria monocytogenes* and the associated microbiome from naturally contaminated ice cream linked to a listeriosis outbreak. BMC Microbiol. 16, 275 (2016). [PubMed: 27852235]
67. Ponnusamy D et al. Cross-talk among flesh-eating *Aeromonas hydrophila* strains in mixed infection leading to necrotizing fasciitis. Proc. Natl Acad. Sci. USA 113, 722–727 (2016). [PubMed: 26733683]
68. Hasan NA et al. Microbial community profiling of human saliva using shotgun metagenomic sequencing. PLoS ONE 9, e97699 (2014). [PubMed: 24846174]
69. Lax S et al. Longitudinal analysis of microbial interaction between humans and the indoor environment. Science 345, 1048–1052 (2014). [PubMed: 25170151]
70. Hatano S et al. Development of a new monoclonal antibody specific to mouse Vγ6 chain. Life Sci. Alliance 2, e201900363 (2019). [PubMed: 31064767]

71. Wang G et al. Arf1-mediated lipid metabolism sustains cancer cells and its ablation induces anti-tumor immune responses in mice. Nat. Commun 11, 220 (2020). [PubMed: 31924786]

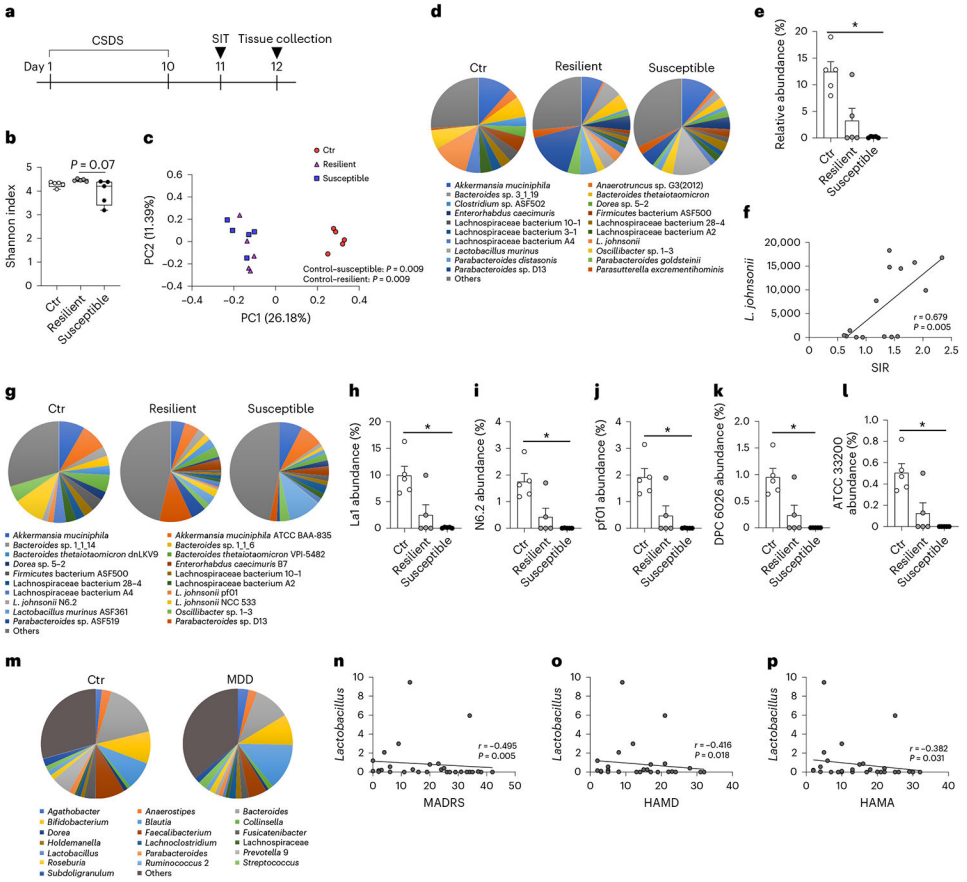

Fig. 1 |. Alteration of intestinal microbiota correlates with social avoidance in CSDS mice as well as disease severity in patients with MDD.

a, Schematic of the experimental design. Eight-week-old C57BL/6 mice were exposed to CSDS for 10 d, followed by a three-chamber social interaction test (SIT) to define susceptible and resilient phenotypes using their social interaction ratio (SIR) score; tissues including fecal samples, colon, small intestine, spleen and meninges were subsequently collected. **b**,**c**, Shannon α-diversity (**b**) and Jaccard β-diversity (**c**) indices of grouped data of fecal bacteria of CSDS mice at the species level. **c**, PC, principal component. **d**, Relative abundance of fecal bacteria of control, resilient and susceptible mice at the species level. **e**, Relative abundance of *L. johnsonii* in the feces of control, resilient and susceptible mice. **f**, Spearman's correlation analysis (two-tailed) showing the correlation between the relative abundance of *L. johnsonii* and SIR ($n = 15$). **g**, Relative abundance of fecal bacteria of control, resilient and susceptible mice at the strain level. **d**,**g**, For details on the altered species across conditions, refer to Supplementary Table 1. **h**–**l**, Relative abundance of the fecal *L. johnsonii* strains La1 (**h**), N6.2 (**i**), pf01 (**j**), DPC 6026 (**k**) and ATCC 33200 (**l**) in control, resilient and susceptible mice. **b**–**e**,**g**–**l**, $n = 5$ for all groups. **m**, Relative abundance of fecal bacteria from patients with MDD ($n = 32$) and healthy controls ($n = 34$) at the genus level. The fecal microflora were analyzed by *16S* rRNA gene sequencing. **n**–**p**, Spearman's correlation analysis (two-tailed) showing the correlation between the relative abundance of *Lactobacillus* at the genus level and three clinical assessment scores in patients with MDD ($n = 32$)–that is, MADRS (**n**), HAMD (**o**) and HAMA (**p**). **f**,**n**–**p**, *r*, coefficient of multiple

correlation. **b**, Box plots indicate the value of median (horizontal line), the 25th to 75th percentiles (box) and the minimum–maximum range (whisker) of the values. *$P < 0.05$; P values were determined using a one-way analysis of variance (ANOVA) with Tukey's post-hoc test; adjustments were made for multiple comparisons; **e**, $P = 0.021$; **h**, $P = 0.034$; **i**, $P = 0.039$; **j**, P = 0.034; **k**, $P = 0.037$; and **l**, $P = 0.044$. Data are the mean ± s.e.m.

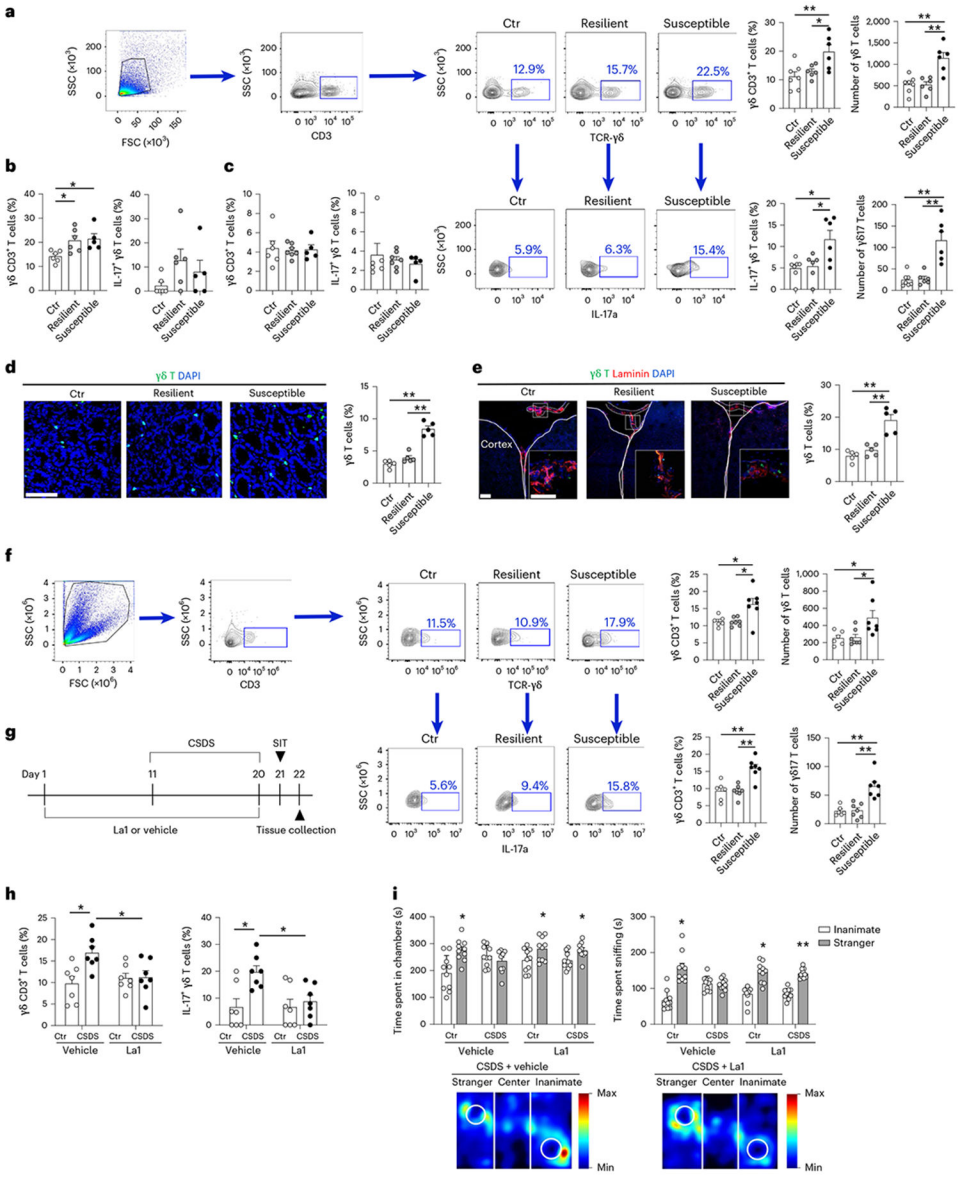

Fig. 2 |. Increase and differentiation of γδ T cells in the colon and meninges of susceptible mice.

a, Representative flow cytometry plots of $CD3^+$, γδ ($CD3^+TCR\text{-}γδ^+$) and γδ17 ($CD3^+TCR\text{-}γδ^+IL\text{-}17^+$) T cells in the LP of the colon. The percentages of cells in the blue quadrants are indicated. The graphs represent the percentage (top left) and number (top right) of γδ T cells as well as the percentage (bottom left) and number (bottom right) of γδ17 T cells in the LP of the colon of control, resilient and susceptible mice ($n = 7$, 6 and 6, respectively). **b**,**c**, Percentage of γδ (left) and γδ17 (right) T cells in the LP of the small intestine (**b**; $n = 6$, 6 and 5 mice, respectively) and spleen (**c**) ($n = 6$, 7 and 5 mice, respectively) of control, resilient and susceptible mice. **d**, Immunohistochemistry of TCR-γδ and 4′,6-diamidino-2-phenylindole (DAPI) in the colon (left). Percentage of $TCR\text{-}γδ^+$ cells (relative to total cells) in the colon of control, resilient and susceptible mice (right). **e**, Immunohistochemistry of TCR-γδ, laminin and DAPI in the coronal brain section (left). The dotted line is an outline of meninges. Insets: magnified views of the regions

in the main images outlined by white squares. Percentage of TCR-$\gamma\delta^+$ cells (relative to total cells) in the meninges of control, resilient and susceptible mice. **d**,**e**, Scale bars, 50 μm; $n = 5$ for all groups. **f**, Representative flow cytometry plots of $CD3^+$, γδ and γδ17 T cells in the meninges. The graphs represent the percentage (top left) and number (top right) of γδ T cells as well as the percentage (bottom left) and number (bottom right) of γδ17 T cells in the meninges of control, resilient and susceptible mice ($n = 6$, 7 and 7, respectively). **g**, Schematic of the *L. johnsonii* La1 treatment experiments. SIT, social interaction test. **h**, Percentage of γδ (left) and γδ17 (right) T cells in the LP of the colon of control and CSDS mice treated with or without La1 ($n = 7$ for all groups). **i**, CSDS-induced sociability phenotypes of control + vehicle, CSDS + vehicle, control + La1 and CSDS + La1 mice ($n = 10$, 10, 10 and 9, respectively). Time spent in the chamber with (top left) and sniffing (top right) an inanimate object or stranger. Representative heatmaps depicting mouse movements (bottom); white circles are the outlines of plastic cages holding a stranger mouse or inanimate object. Min, minimum; max, maximum. $^*P < 0.05$ and $^{**}P < 0.01$; *P* values were determined using a one-way (**a**–**f**) or two-way (**h**) ANOVA with Tukey's post-hoc test, or an unpaired two-tailed Student's *t*-test (**i**); **a**, γδ T cell percentage: $P = 0.0083$ and $P = 0.0436$; γδ T cell number, $P = 0.0007$ and $P = 0.0009$; γδ17 T cell percentage, $P = 0.0113$ and $P = 0.0227$; and γδ17 T cell number, $P = 0.0001$ and $P = 0.0003$; **b**, $P = 0.031$ and $P = 0.0402$; **d**, $P < 0.0001$ for both comparisons; **e**, $P < 0.0001$ and $P = 0.0004$; **f**, γδ T cell percentage, $P = 0.0177$ and $P = 0.0112$; γδ T cell number, $P = 0.0305$ and $P = 0.0293$; γδ17 T cell percentage, $P = 0.0006$ and $P = 0.0004$; and γδ17 T cell number, $P = 0.0003$ and $P = 0.0002$; **h**, γδ T cell percentage, $P = 0.0102$ and $P = 0.0488$; and γδ17 T cell percentage, $P = 0.0113$ and $P = 0.0406$; **i**, Time spent in chambers, $P = 0.0468$, $P = 0.044$ and $P = 0.0219$; time spent sniffing, $P = 0.0251$, $P = 0.0266$ and $P = 0.0007$. Data are the mean ± s.e.m. Ctr, control.

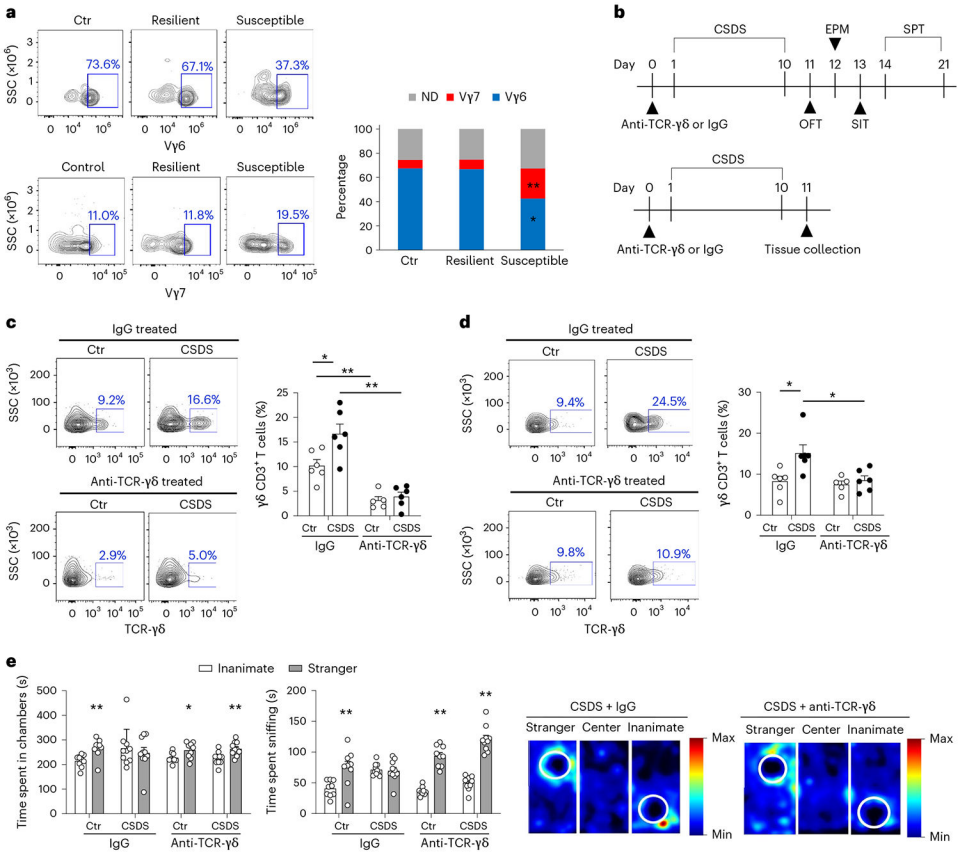

Fig. 3 |. Inhibition of peripheral γδ T cells blocks CSDS-induced social avoidance.

a, Representative flow cytometry plots (left) and the percentage of Vγ6$^+$ and Vγ7$^+$ γδ T cell subpopulations (right) in the meningeal γδ T cells of control, resilient and susceptible mice (n = 7 for all groups). The percentages of cells in the blue quadrants are indicated. ND, not determined. **b**, Schematic of the experimental design. Eight-week-old C57BL/6 mice received an i.p. injection of monoclonal antibody to TCR-γδ or its isotype control 1 d before being exposed to 10 d of CSDS; exposure was followed by an open field (OFT), elevated plus maze (EPM) and social interaction (SIT; top) test or a sucrose preference test (SPT; bottom) from an independent cohort of mice treated with anti-TCR-γδ or IgG; tissues were harvested 1 d after CSDS. **c**,**d**, Representative flow cytometry plots of γδ T cells (CD3$^+$TCR-γδ$^+$; left) and the percentage of the γδ T cells, relative to total CD3$^+$ T cells, in the LP of the colon (**c**) and meninges (**d**) of control + IgG, CSDS + IgG, control + anti-TCR-γδ and CSDS + anti-TCR-γδ mice (n = 6, 6, 5 and 6, respectively). The blue boxes in the dot plots identify γδ T cells or γδ17 T cells, and the percentage of γδ T cells in CD3$^+$ T cells or γδ17 T cells in γδ T cells in each group are indicated above the boxes. **e**, Sociability phenotypes of control + IgG, CSDS + IgG, control + anti-TCR-γδ and CSDS + anti-TCR-γδ mice (n = 9, 10, 9 and 10, respectively). Time spent in the chamber with (top left) and sniffing (top right) an inanimate object or stranger. Representative heatmaps depict mouse movements (bottom); white circles are the outlines of plastic cages holding a stranger mouse or inanimate object. Min, minimum; max, maximum. *P < 0.05 and **P < 0.01; P values were determined using a one-way (**a**) or two-way (**c**,**d**) ANOVA with

Tukey's post-hoc test, or an unpaired two-tailed Student's *t*-test (**e**); **a**, $^{**}P = 0.0024$ and $^{*}P = 0.0351$; **c**, $P = 0.0127$, $P = 0.0094$ and $P < 0.0001$; **d**, $P = 0.0117$ and $P = 0.0154$; **e**, time spent in chambers, $P = 0.0039$, $P = 0.0273$ and $P = 0.0055$; time spent sniffing, $P = 0.0061$, $P < 0.0001$ and $P < 0.0001$. Data are the mean ± s.e.m. Ctr, control.

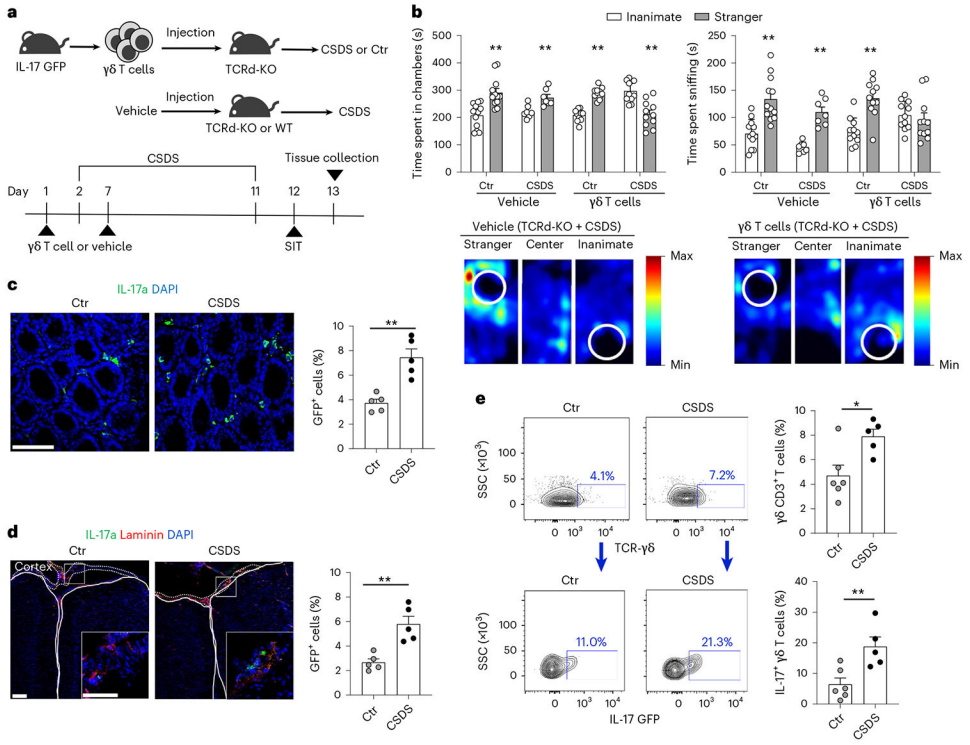

Fig. 4 |. Peripheral γδ17 T cell differentiation contributes to CSDS-induced social avoidance.
a, Schematic of the experimental design. Eight-week-old *Tcrd*$^{-/-}$ (TCRd-KO) mice were i.v. injected with vehicle or γδ T cells collected from IL-17 GFP mice 1d before and 5d after the start of CSDS, which was followed by a social interaction test (SIT) and tissue collection. **b**, Sociability phenotypes of four groups of TCRd-KO mice: control (ctr) + vehicle, CSDS + vehicle, ctr + γδ T cells and CSDS + γδ T cells (n = 12, 7, 11 and 11, respectively). Time spent in the chamber with (top left) and sniffing (top right) an inanimate object or stranger. Representative heatmaps depict mouse movements (bottom); white circles are the outlines of plastic cages holding a stranger mouse or inanimate object. Min, minimum; max, maximum. **c**, Immunohistochemistry of exogenously administered GFP$^+$ γδ17 T cells (green) in the colon of TCRd-KO mice (left). Percentage of GFP$^+$ γδ17 T cells, relative to total cells, in the colon of TCRd-KO mice with ctr + γδ T cells or CSDS + γδ T cells (right). **d**, Immunohistochemistry of exogenously administered GFP$^+$ γδ17 T cells (green), laminin and DAPI in coronal brain sections (left). Percentage of GFP$^+$ γδ17 T cells, relative to total cells, in the meninges of TCRd-KO mice with ctr + γδ T cells or CSDS + γδ T cells (right). **c**,**d**, Scale bars, 50 μm; $n = 5$ for all groups. **e**, Representative flow cytometry plots of γδ (CD3$^+$TCR-γδ$^+$) and γδ17 (CD3$^+$TCR-γδ$^+$IL-17$^+$) T cells (left) as well as the determined percentages γδ T cells in the CD3$^+$ T cell subpopulation (top right) and γδ17 T cells in the γδ T cell subpopulation (bottom right) of the meninges of TCRd-KO mice with ctr + γδ T cells or CSDS + γδ T cells ($n = 6$ and 5, respectively). The percentages of cells in the blue quadrants are indicated. *$P < 0.05$ and **$P < 0.01$; P values were determined using an unpaired two-tailed Student's t-test (**b**–**e**); **b**, time spent in chambers, $P = 0.0005$, $P = 0.0041$, $P < 0.0001$ and $P = 0.0002$; and time spent sniffing, $P = 0.0002$, $P < 0.0001$ and $P =$

0.0001; **c**, $P = 0.0012$; **d**, $P = 0.0022$; **e**, percentage of γδ T cells, $P = 0.0164$; and percentage of γδ17 T cells, $P = 0.0081$. Data are the mean ± s.e.m.

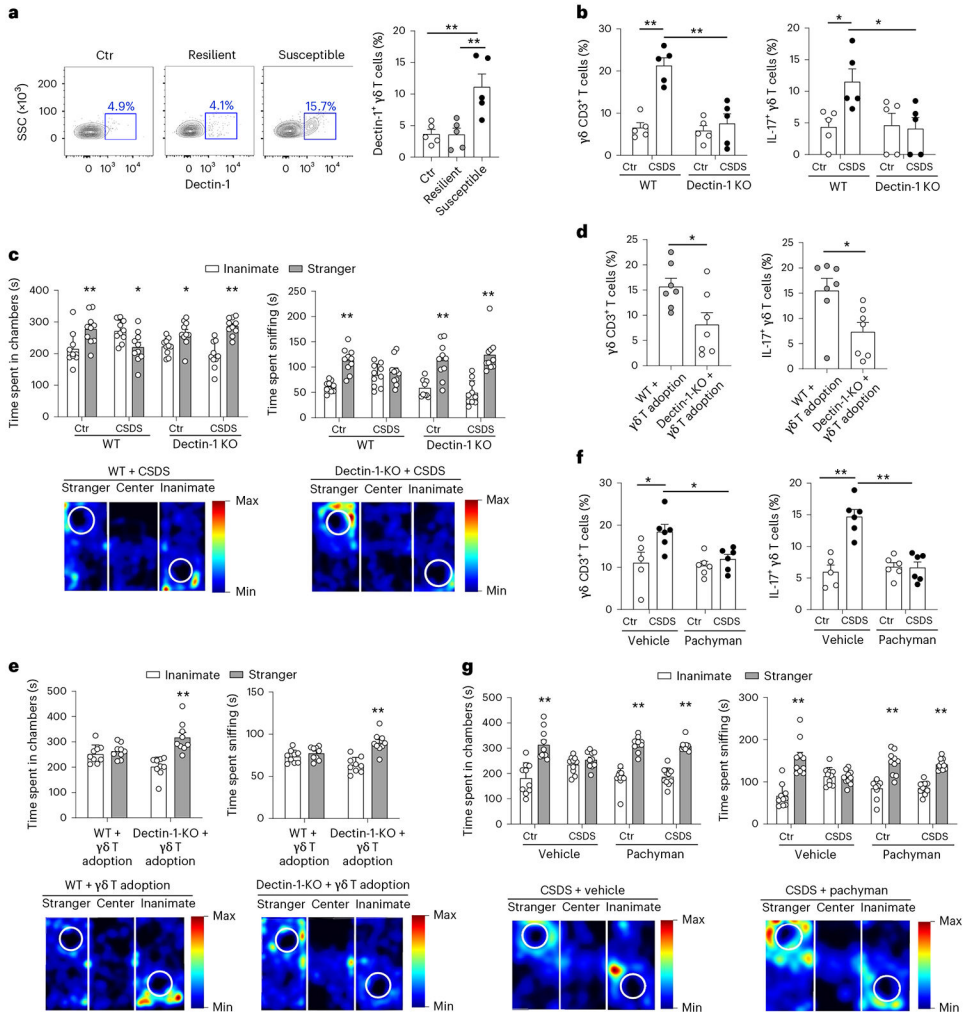

Fig. 5 | Dectin-1 mediates increased colonic γδ T cell populations and γδ17 T cell differentiation as well as the social avoidance induced by CSDS.

a, Representative flow cytometry plots of the dectin-1$^+$ subpopulations of γδ T cells (left). The percentages of cells in the blue quadrants are indicated. Percentage of dectin-1$^+$ γδ T cells in the LP of the colon of control (ctr), resilient and susceptible mice. **b**, Percentage of γδ (left) and γδ17 (right) T cell subpopulations of CD3$^+$ and γδ T cells, respectively, in the LP of the colon of WT + ctr, WT + CSDS, dectin-1 KO + ctr and dectin-1 KO + CSDS mice. **a**,**b**, $n = 5$ for all groups. **c**, CSDS-induced sociability phenotypes of WT + ctr, WT + CSDS, dectin-1 KO + ctr and dectin-1 KO + CSDS mice ($n = 9$, 10, 10 and 10, respectively). **d**, Percentage of γδ (left) and γδ17 (right) T cells in the LP of the colon of TCRd-KO mice subjected to CSDS with WT or dectin-1-KO γδ T cell adoption ($n = 7$ for both groups). **e**, CSDS-induced sociability phenotypes of TCRd-KO mice subjected to CSDS with WT or dectin-1-KO γδ T cell adoption ($n = 9$ for both groups). **f**, Percentage of γδ (left) and γδ17 (right) T cells in the LP of the colon of ctr + vehicle, CSDS + vehicle, ctr + pachyman and CSDS + pachyman mice ($n = 5$, 6, 6 and 6, respectively). **g**, CSDS-induced sociability phenotypes of ctr + vehicle, CSDS + vehicle, ctr + pachyman and CSDS + pachyman mice ($n = 10$ for all groups). **c**,**e**,**g**, Time spent in the chamber with

(top left) and sniffing (top right) an inanimate object or stranger. Representative heatmaps depict mouse movements (bottom); white circles are the outlines of plastic cages holding a stranger mouse or inanimate object. Min, minimum; max, maximum. *$P < 0.05$ and **$P < 0.01$; P values were determined using a one-way (**a**) or two-way (**b**,**f**) ANOVA with Tukey's post-hoc test, or an unpaired two-tailed Student's t-test (**c**–**e**,**g**); **a**, $P = 0.006$ and $P = 0.0056$; **b**, percentage of γδ T cells, $P < 0.0001$ and $P = 0.0002$; percentage of γδ17 T cells, $P = 0.0494$ and $P = 0.0402$; **f**, percentage of γδ T cells, $P = 0.0256$ and $P = 0.0425$; percentage of γδ17 T cells, $P < 0.0001$ for both comparisons; **c**, time spent in chambers, $P = 0.0039$, $P = 0.0142$, $P = 0.0122$ and $P < 0.0001$; time spent sniffing, $P < 0.0001$, $P = 0.0004$ and $P < 0.0001$; **d**, percentage of γδ T cells, $P = 0.0236$; percentage of γδ17 T cells, $P = 0.02$; **e**, time spent in chambers, $P = 0.0001$; time spent sniffing, $P < 0.0001$; and **g**, time spent in chambers, $P = 0.0001$, $P < 0.0001$ and $P < 0.0001$; time spent sniffing, $P < 0.0001$ for all comparisons. Data are the mean ± s.e.m.

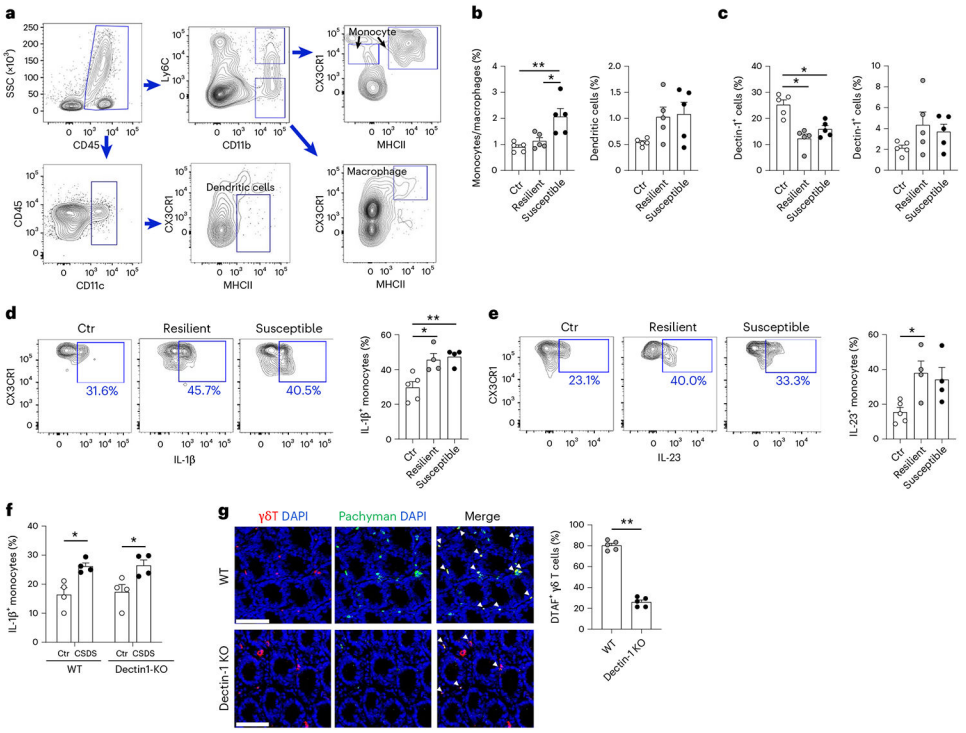

Fig. 6 |. CSDS-induced colonic IL-1β production in myeloid cells is independent of dectin-1 signaling.

a, Representative flow cytometry plots of monocytes (top right), macrophages (bottom right) and dendritic cells (bottom middle) in the LP of the colon. **b**, Percentage of monocytes/macrophage (left) and dendritic (right) cell subpopulations of $CD45^+$ cells in the LP of the colon of control, resilient and susceptible mice. **c**, Percentage of dectin-1^+ cells in monocytes/macrophages (left) and dendritic cells (right) in the LP of the colon of control, resilient and susceptible WT mice. **d**,**e**, Representative flow cytometry plots of IL-1β- (**d**) and IL-23-producing (**e**) monocytes in the LP of the colon (left). The percentages of cells in the blue quadrants are indicated. Calculated percentages of these cell populations in control, resilient and susceptible mice (n = 5, 4 and 4, respectively). **f**, Percentage of IL-1β-producing cell subpopulations of monocytes in the LP of the colon of WT + ctr, WT + CSDS, dectin-1 KO + ctr and dectin-1 KO + CSDS mice (n = 4 for all groups). **g**, Immunohistochemical analysis of orally administered fluorescein DTAF-labeled pachyman γδ T cells in the colon. The white arrowheads indicate co-localization of green and red signals. Scale bars, 50 μm. Percentage of DTAF-labeled γδ T cells in the colon of WT and dectin-1-KO mice. **b**,**c**,**g**, n = 5 for all groups. *P < 0.05 and **P < 0.01; P values were determined using a one-way (**b**–**e**) or two-way (**f**) ANOVA with Tukey's post-hoc test, or an unpaired two-tailed Student's t-test (**g**); **b**, P = 0.0037 and P = 0.0164; **c**, P = 0.0052 and P = 0.0004; **d**, P = 0.0076 and P = 0.0143; **e**, P = 0.036; **f**, P = 0.028 and P = 0.0393; and **g**, P < 0.0001. Data are the meant ± s.e.m. Ctr, control.